

DOI: 10.1002/cmdc.201402310

# Design and Synthesis of Imidazo[2,1-*b*]thiazole–Chalcone Conjugates: Microtubule-Destabilizing Agents

Ahmed Kamal,<sup>\*[a, b]</sup> Moku Balakrishna,<sup>[a]</sup> V. Lakshma Nayak,<sup>[a]</sup> Thokhir Basha Shaik,<sup>[a]</sup> Shaikh Faazil,<sup>[a]</sup> and Vijaykumar D. Nimbarte<sup>[b]</sup>

A series of chalcone conjugates featuring the imidazo[2,1-*b*]thiazole scaffold was designed, synthesized, and evaluated for their cytotoxic activity against five human cancer cell lines (MCF-7, A549, HeLa, DU-145 and HT-29). These new hybrid molecules have shown promising cytotoxic activity with IC<sub>50</sub> values ranging from 0.64 to 30.9 μM. Among them, (*E*)-3-(6-(4-fluorophenyl)-2,3-bis(4-methoxyphenyl)imidazo[2,1-*b*]thiazol-5-yl)-1-(pyridin-2-yl)prop-2-en-1-one (**11 x**) showed potent antiproliferative activity with IC<sub>50</sub> values ranging from 0.64 to 1.44 μM in all tested cell lines. To investigate the mechanism of action, the detailed biological aspects of this promising conju-

gate (**11 x**) were carried out on the A549 lung cancer cell line. The tubulin polymerization assay and immunofluorescence analysis results suggest that this conjugate effectively inhibits microtubule assembly in A549 cells. Flow cytometric analysis revealed that this conjugate induces cell-cycle arrest in the G2/M phase and leads to apoptotic cell death. This was further confirmed by Hoechst staining, activation of caspase-3, DNA fragmentation analysis, and Annexin V–FITC assay. Moreover, molecular docking studies indicated that this conjugate (**11 x**) interacts and binds efficiently with the tubulin protein.

## Introduction

Antimitotic agents constitute an importance class of drugs used in the treatment of cancer. They usually target tubulin thereby inhibiting the formation of the mitotic spindle.<sup>[1]</sup> α,β-tubulin heterodimers polymerize to form hollow cylindrical filament structures called microtubules. These are the key components of the cytoskeleton of eukaryotic cells and play a vital role in various cellular functions like intracellular migration and transport, cell shape maintenance, polarity, cell signaling, and mitosis.<sup>[2,3]</sup> Inhibiting tubulin polymerization or interfering with microtubule disassembly disrupts several cellular functions, including cell motility and mitosis.<sup>[4–6]</sup> Therefore microtubule dynamics is an important target for developing anticancer drugs.<sup>[7]</sup>

The discovery and development of molecules that affect tubulin polymerization, which is the origin of microtubules, is of immense importance.<sup>[8–10]</sup> Molecules like colchicine (**1**) and combretastatin A-4 (CA-4; **2**) (Figure 1) bind to tubulin thereby inhibiting its polymerization into microtubules. Due to its structural simplicity, ease of synthesis, and potent antitumor

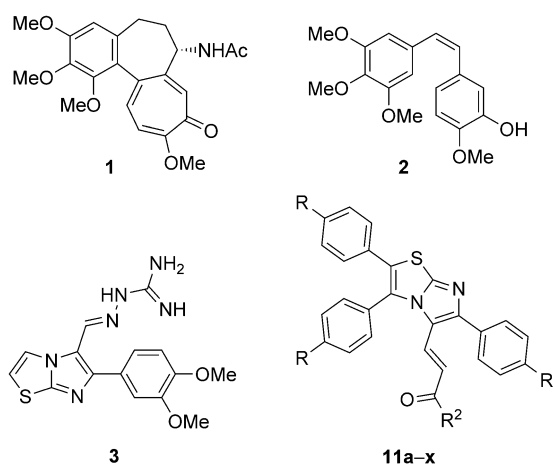


**Figure 1.** Structures of colchicine (**1**), combretastatin A-4 (**2**), imidazo[2,1-*b*]thiazole guanylhydrazone (**3**), and 2,3-diaryl imidazo[1,2-*b*]thiazole chalcones **11 a–x**.

activity, this class of molecules is widely studied to find potent anticancer agents.<sup>[11–13]</sup>

Recently, conjugates bearing imidazo[2,1-*b*]thiazole scaffolds have become of interest due to their broad spectrum of pharmacological activities, such as antifungal,<sup>[14,15]</sup> antibacterial,<sup>[16–18]</sup> anti-inflammatory,<sup>[19]</sup> and antihypertensive properties.<sup>[20]</sup> It has been reported that they possess antitumor properties against a variety of human cancer cell lines.<sup>[21–24]</sup> Imidazo[2,1-*b*]thiazole-guanylhydrazone derivative (**3**) (Figure 1) is a fused imidazo-thiazole compound that showed potent antiproliferative activity against a number of cancer cell lines and is considered as promising drug candidate.

[a] Dr. A. Kamal, M. Balakrishna, V. L. Nayak, T. B. Shaik, S. Faazil  
Medicinal Chemistry & Pharmacology  
Council of Science and Industrial Research  
Indian Institute of Chemical Technology (CSIR–IICT), Hyderabad 500 007  
(India)  
E-mail: ahmedkamal@iict.res.in

[b] Dr. A. Kamal, V. D. Nimbarte  
Department of Medicinal Chemistry  
National Institute of Pharmaceutical Education and Research (NIPER)  
Hyderabad-500 037 (India)

Supporting information for this article is available on the WWW under  
<http://dx.doi.org/10.1002/cmdc.201402310>.

Similarly, chalcones are known to exhibit a wide range of biological activities, such as anti-HIV,<sup>[25a]</sup> tyrosinase inhibition,<sup>[25b]</sup> anti-inflammatory,<sup>[25c]</sup> anti-invasive,<sup>[25d]</sup> antibacterial,<sup>[25e]</sup> and antimalarial.<sup>[25f]</sup> Chalcones are regarded as promising anti-proliferative agents against most human cancers. It is known that they are capable of inducing apoptosis<sup>[26,27]</sup> and also have the capability to uncouple mitochondrial respiration and thus collapse mitochondrial membrane potential.<sup>[28]</sup> They are also effective (in vivo) as cell proliferation inhibitors, anti-tumor-promoting and chemopreventive agents.<sup>[29]</sup>

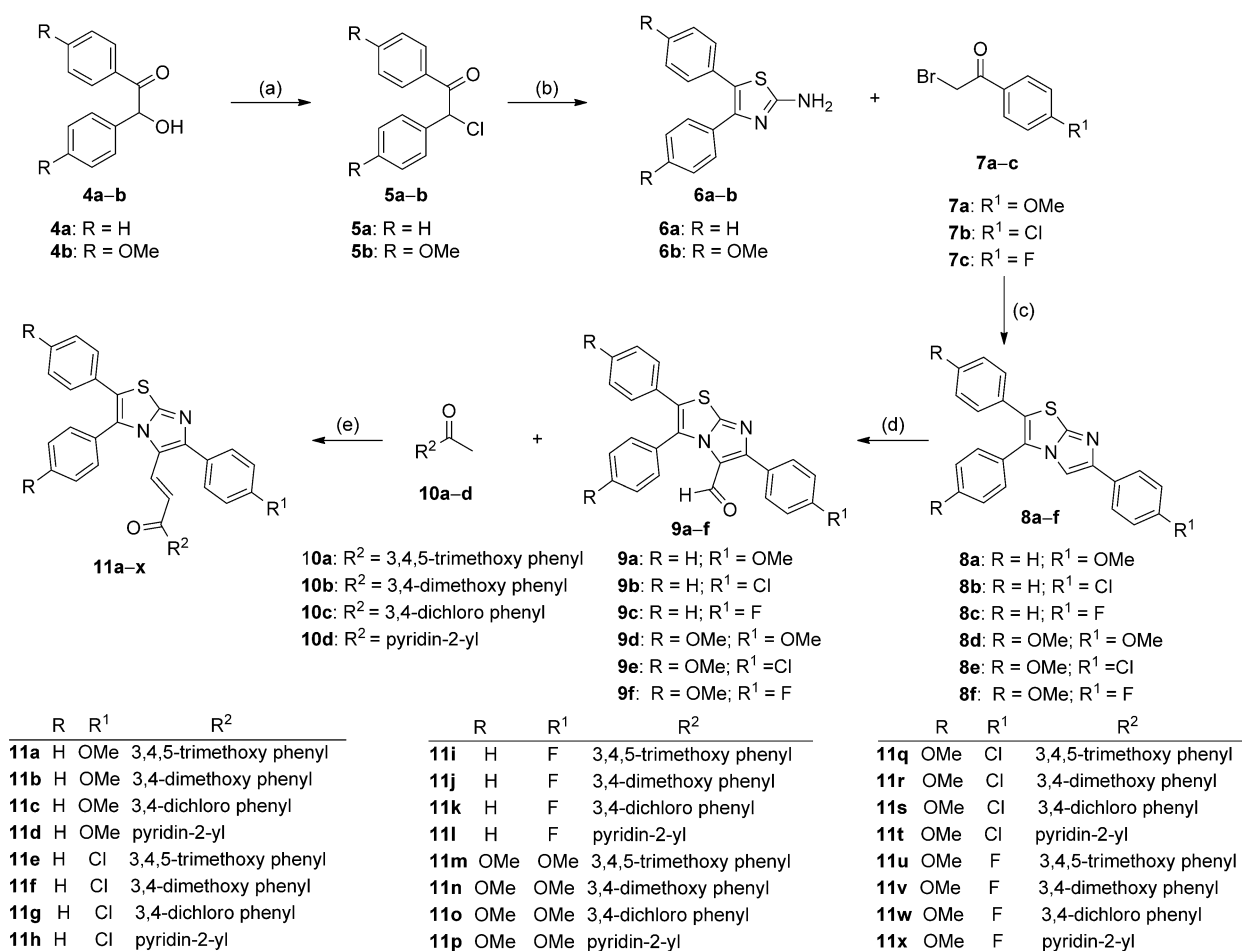
A number of potent hybrid anticancer molecules have been obtained by grouping different pharmacophores.<sup>[30,31]</sup> Continuing our search for newer leads with effective antitumor properties<sup>[32–34]</sup> and considering promising antiproliferative activities of imidazothiazoles and chalcones, we have designed newer conjugates by combining both chalcone and imidazothiazole moieties to enhance their anticancer potential. In this context we have designed and synthesized 2,3-diaryl imidazo[1,2-*b*]thiazole–chalcone conjugates **11 a–x** and evaluated their anticancer activity. Compound **11 x** was found to be the most effective conjugate from the series against the A549 lung cancer cell line. Therefore conjugate **11 x** was selected for further biological investigations. This compound was initially tested for its

effect on the cell cycle and was found to cause arrest in the G2/M phase. Since inhibition of tubulin polymerization is strongly associated with G2/M cell-cycle arrest,<sup>[35]</sup> it was considered of interest to investigate its effect on tubulin polymerization. In addition, several studies to determine the apoptotic effect of **11 x** were also undertaken.

## Results and Discussion

### Chemistry

The 2,3-diaryl imidazo[1,2-*b*]thiazole–chalcone conjugates were synthesized from commercially available benzoin and anisoin, as depicted in Scheme 1. Initially, 2-chloro-1, 2-diarylethanones (**5 a,b**) were prepared from 2-hydroxy-1,2-diarylethanones (**4 a,b**) by treating with thionyl chloride in dichloromethane.<sup>[36]</sup> Compound **5 a** is also commercially available. The 2-chloro-1,2-diarylethanones (**5 a,b**) were converted into 4,5-diaryl-2-aminothiazoles (**6 a,b**) by refluxing with thiourea in ethanol for 15 h. Further, the 2-aminothiazoles (**6 a,b**) were treated with the appropriate bromoketones (**7 a–c**) in propan-2-ol at reflux temperature to afford corresponding imidazo[1,2-*b*]thiazoles (**8 a–f**).<sup>[37]</sup> Next, formylation was carried out at C5 position by the



**Scheme 1.** Reagents and conditions: a) SOCl<sub>2</sub>, CH<sub>2</sub>Cl<sub>2</sub>, 0 °C, 1–2 h, 73–82%; b) thiourea, EtOH, 80 °C, 15 h, 64–67%; c) propan-2-ol, 80 °C, 3 h, 52–60%; d) POCl<sub>3</sub>, DMF, CHCl<sub>3</sub>, reflux, 4 h, 73–86%; e) 10% aq KOH, EtOH, reflux, 8 h, 52–81%.

Vilsmier reaction to obtain 2,3-diphenylimidazo[2,1-*b*]thiazole-5-carbaldehydes (**9a–f**).<sup>[38]</sup> Finally, 2,3-diphenylimidazo[2,1-*b*]thiazole-5-carbaldehydes (**9a–f**) were treated with various acetophenones (**10a–d**) under the Claisen–Schmidt condensation conditions to furnish 2,3-diaryl imidazo[1,2-*b*]thiazole-chalcone conjugates (**11a–x**).<sup>[39]</sup>

## Biological evaluation

### Antiproliferative activity

These conjugates (**11a–x**) were evaluated for their antiproliferative activity in a panel of five human cancer cell lines, namely MCF-7 (breast), A549 (lung), HeLa (cervix), DU-145 (prostate), and HT-29 (colon) by employing an MTT cell viability assay<sup>[40,41]</sup> with doxorubicin as the reference drug. The results are summarized in Table 1 and expressed as IC<sub>50</sub> values. The results revealed that these conjugates exhibit promising antiproliferative activity with IC<sub>50</sub> values ranging from 0.64 to 30.9 μM against the tested cell lines. Conjugate **11x** showed significant activity against the five human cancer cell lines. Among the tested cancer cell lines, A549 cells were the most sensitive to **11x** with an IC<sub>50</sub> value of 0.64 μM. Therefore, A549 was chosen as a model cell line for subsequent experiments.

### Cell-cycle analysis

Anticancer agents generally alter the regulation of the cell cycle resulting in the arrest of cell division in various phases, thereby decreasing the growth and proliferation of cancerous cells. The results of the cytotoxicity assay suggest that conjugate **11x** possesses significant antiproliferative activity against the human lung cancer cell line A549. The promising activity of **11x** prompted us to examine its influence on cell-cycle progression.

A549 cells were treated with nocodazole (1 μM) and conjugate **11x** (0.5 and 1 μM) for 24 h. After treatment with the conjugate, it was observed that the percentage of cells in the G0/G1 phase decreased and accumulation of cells in the G2/M phase increased in a dose-dependent manner. Finally, cell-cycle analysis confirmed that the antiproliferative activity of this conjugate was related to cell-cycle arrest in the G2/M phase (Figure 2). These data clearly indicate that **11x** could be considered as a mitosis-blocking agent.

### Effect on inhibition of tubulin polymerization

Tubulin-binding molecules interfere with the dynamic stability of microtubules and thereby induce cell-cycle arrest in the M phase and formation of abnormal mitotic spindles resulting in apoptotic cell death.<sup>[42]</sup> Conjugates that eventually alter cell-cycle parameters with preference to G2/M blockade are known to exhibit effects on tubulin assembly.

The progression of tubulin polymerization<sup>[43,44]</sup> was thus examined by monitoring the increase in fluorescence emission at 420 nm (excitation at 360 nm) in a 384-well plate for 1 h at 37 °C with and without the conjugates at 3 μM in comparison with nocodazole (a known tubulin inhibitor). The MTT assay results revealed that conjugates **11i**, **11v**, **11w** and **11x** showed significant antiproliferative activity against A549 cells. In this context, a tubulin polymerization assay was performed. Among the four conjugates examined, **11x** inhibited tubulin polymerization by 65.36% (Figure 3). Moreover, compound **11x** showed potent inhibition of tubulin polymerization with an IC<sub>50</sub> value of 1.43 μM, whereas nocodazole exhibited an IC<sub>50</sub> value of 1.25 μM (Table 2).

Compd	IC <sub>50</sub> [μM] <sup>[a]</sup>				
	MCF-7 <sup>[b]</sup>	A549 <sup>[c]</sup>	HeLa <sup>[d]</sup>	DU-145 <sup>[e]</sup>	HT-29 <sup>[f]</sup>
<b>11a</b>	7.94 ± 0.004	6.91 ± 0.11	13.0 ± 0.44	7.58 ± 0.12	15.8 ± 0.25
<b>11b</b>	8.31 ± 0.3	13.9 ± 0.18	15.8 ± 0.52	18.1 ± 0.41	23.6 ± 0.08
<b>11c</b>	5.62 ± 0.09	5.49 ± 0.18	11.5 ± 0.37	4.78 ± 0.08	6.30 ± 0.10
<b>11d</b>	5.75 ± 0.56	1.58 ± 0.36	7.94 ± 0.26	6.02 ± 0.10	3.98 ± 0.13
<b>11e</b>	25.1 ± 9.69	7.07 ± 0.39	13.5 ± 0.17	15.1 ± 0.08	30.2 ± 3.58
<b>11f</b>	28.8 ± 0.37	11.0 ± 1.31	20.8 ± 0.10	12.7 ± 0.84	18.4 ± 0.32
<b>11g</b>	8.55 ± 1.15	3.80 ± 0.18	11.2 ± 1.10	3.71 ± 0.06	6.96 ± 0.05
<b>11h</b>	4.16 ± 0.27	2.57 ± 0.09	7.41 ± 0.61	4.67 ± 0.23	3.54 ± 0.75
<b>11i</b>	1.94 ± 0.10	0.97 ± 0.22	2.88 ± 0.29	1.28 ± 0.10	3.38 ± 0.76
<b>11j</b>	1.86 ± 1.44	1.47 ± 0.37	3.01 ± 0.20	1.59 ± 0.03	4.89 ± 0.25
<b>11k</b>	3.16 ± 0.36	4.89 ± 0.16	5.62 ± 0.18	7.41 ± 0.12	6.91 ± 0.78
<b>11l</b>	2.29 ± 0.07	1.23 ± 0.03	4.78 ± 0.24	1.58 ± 0.09	1.99 ± 0.35
<b>11m</b>	1.90 ± 0.06	4.78 ± 0.85	8.12 ± 0.56	8.12 ± 0.39	7.76 ± 0.76
<b>11n</b>	18.2 ± 0.1	9.77 ± 1.63	31.6 ± 6.89	9.33 ± 0.15	12.3 ± 0.20
<b>11o</b>	5.37 ± 0.17	8.91 ± 0.79	7.94 ± 0.26	8.31 ± 0.27	5.01 ± 0.24
<b>11p</b>	2.51 ± 0.12	1.51 ± 0.01	7.76 ± 0.13	2.63 ± 0.08	8.31 ± 0.35
<b>11q</b>	14.3 ± 0.50	16.6 ± 1.13	9.33 ± 0.15	13.4 ± 0.59	25.0 ± 0.43
<b>11r</b>	10.4 ± 1.53	12.88 ± 0.28	15.8 ± 1.11	28.0 ± 2.37	26.8 ± 2.28
<b>11s</b>	22.7 ± 5.37	9.95 ± 0.16	30.9 ± 5.53	17.8 ± 0.01	26.6 ± 6.72
<b>11t</b>	2.63 ± 0.81	1.77 ± 0.37	9.46 ± 1.08	2.34 ± 0.35	5.49 ± 0.98
<b>11u</b>	2.03 ± 0.36	1.81 ± 0.60	2.51 ± 0.37	4.07 ± 0.06	6.91 ± 0.11
<b>11v</b>	2.34 ± 1.17	0.92 ± 0.06	6.91 ± 0.23	1.31 ± 0.09	2.18 ± 0.04
<b>11w</b>	1.09 ± 0.24	0.73 ± 0.61	3.01 ± 0.05	1.18 ± 0.54	2.23 ± 0.29
<b>11x</b>	0.93 ± 0.04	0.64 ± 0.17	1.44 ± 0.02	1.05 ± 0.03	1.31 ± 0.13
Doxorubicin	1.41 ± 0.74	1.06 ± 0.19	0.92 ± 0.29	1.65 ± 0.03	0.81 ± 0.23

[a] Half maximal inhibitory concentration (IC<sub>50</sub>); values are the mean ± standard deviation (SD) of three independent experiments performed in triplicate determined after 48 h of treatment. [b] Breast cancer. [c] Lung cancer. [d] Cervical cancer. [e] Prostate cancer. [f] Colon cancer.

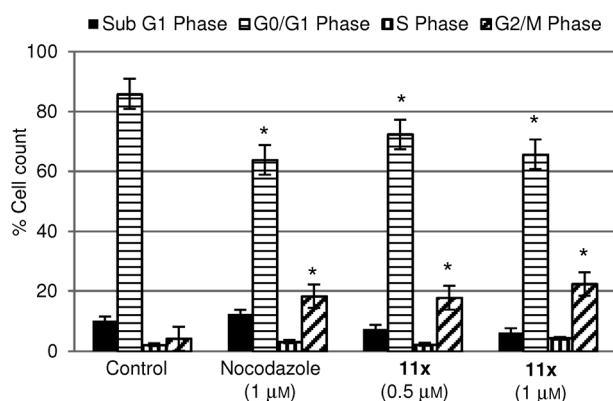


**Figure 2.** Effect of conjugate on cell-cycle progression of A549 cells. Data are expressed as the cell count (%) in each phase of the cell cycle induced by each compound. Values are the mean  $\pm$  standard deviation (SD) of two independent experiments performed in triplicate. Statistical analysis was performed using GraphPad Prism software version 5.01. (\* $p < 0.05$  vs. control).

Compd	IC <sub>50</sub> [ $\mu$ M] <sup>[a]</sup>
<b>11i</b>	2.11 $\pm$ 0.07
<b>11v</b>	2.09 $\pm$ 0.36
<b>11w</b>	1.65 $\pm$ 0.30
<b>11x</b>	1.43 $\pm$ 0.06
Nocodazole	1.25 $\pm$ 0.15

[a] Concentration of compound required to inhibit 50% of tubulin assembly (IC<sub>50</sub>); values are the mean  $\pm$  standard deviation (SD) of two independent experiments performed in triplicate. Statistical analysis was performed using GraphPad Prism software version 5.01.

### Competitive tubulin-binding assay

As compound **11x** showed similar inhibitory effects on tubulin polymerization compared with nocodazole, it was considered of interest to investigate its binding site on tubulin; hence, a fluorescence-based assay was carried out.<sup>[45]</sup> The tubulin–colchicine complex gives a fluorescence signal at 435 nm when excited at 350 nm. Tubulin–colchicine complex fluorescence was monitored at 435 nm when excited at 350 nm in the presence and absence of the test compound (**11x**). Nocodazole was used as a positive control and paclitaxel as a negative control. A remarkable decrease in complex fluorescence was observed when tubulin and colchicine were co-incubated with **11x** at 37 °C for 60 min compared with nocodazole. Paclitaxel exerts no effect on the complex fluorescence as it binds at a different site on tubulin (Figure 4). These observations indicate that both **11x** and nocodazole inhibit the binding of colchicine to tubulin, thereby suggesting that **11x** binds at the colchicine binding site.

### Immunohistochemistry studies on tubulin

In addition to in vitro tubulin polymerization studies, we investigated alterations in the microtubule network in A549 cells in-

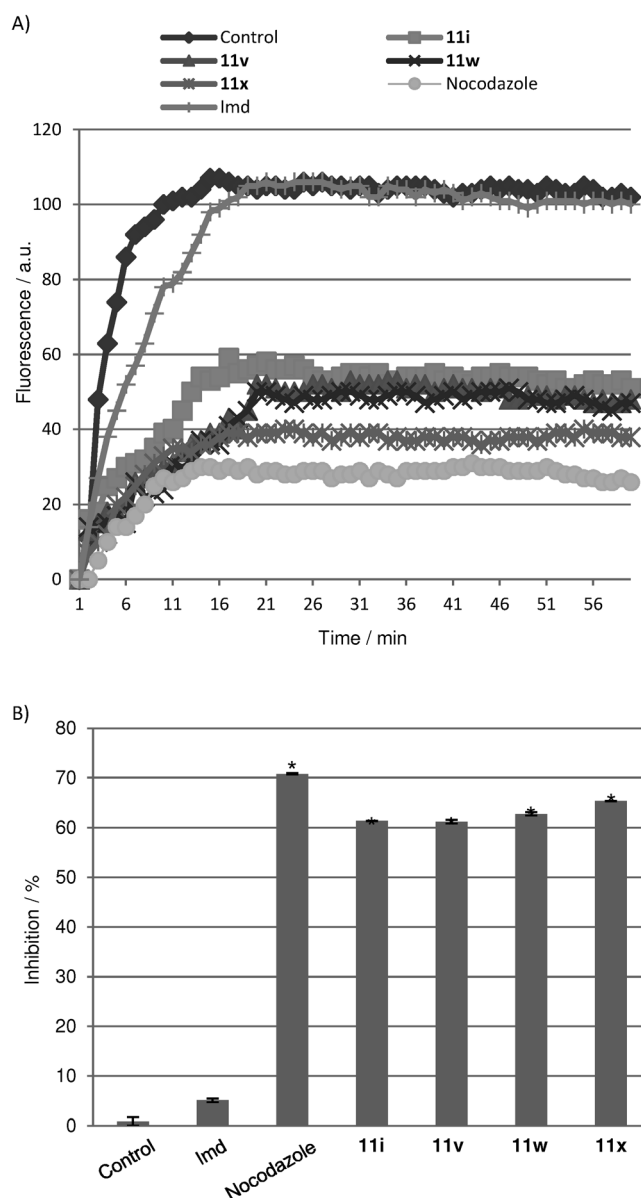


**Figure 3.** Effect of conjugates on tubulin polymerization. Tubulin polymerization was monitored by the increase in fluorescence at 360 nm (excitation) and 420 nm (emission) for 1 h at 37 °C. All conjugates were tested at a final concentration of 3  $\mu$ M. Nocodazole was used as a positive control. Values are the mean  $\pm$  standard deviation (SD) of two independent experiments performed in triplicate. Statistical analysis was performed using GraphPad Prism software version 5.01. (\* $p < 0.05$  vs. control).

duced by conjugate **11x** by using confocal microscopy of immunohistochemistry studies, as most antimitotic agents affect microtubules.<sup>[46]</sup> Therefore, A549 cells were treated with **11x** (0.5 and 1  $\mu$ M) for 24 h. The results demonstrated a well-organized microtubular network in control cells. However, cells treated with **11x** and nocodazole showed disrupted microtubule organization as seen in Figure 5, thus confirming the inhibition of tubulin polymerization.

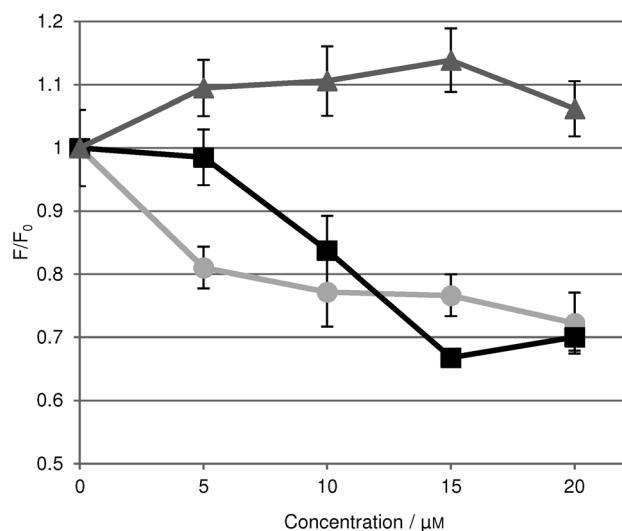


**Figure 4.** Colchicine competition binding assay results showing that conjugate **11x** competitively binds to the colchicine binding site of tubulin (● **11x**; ■ nocodazole; ▲ paclitaxel). The assay was performed in duplicate, and the experiment was repeated twice; representative data are shown.

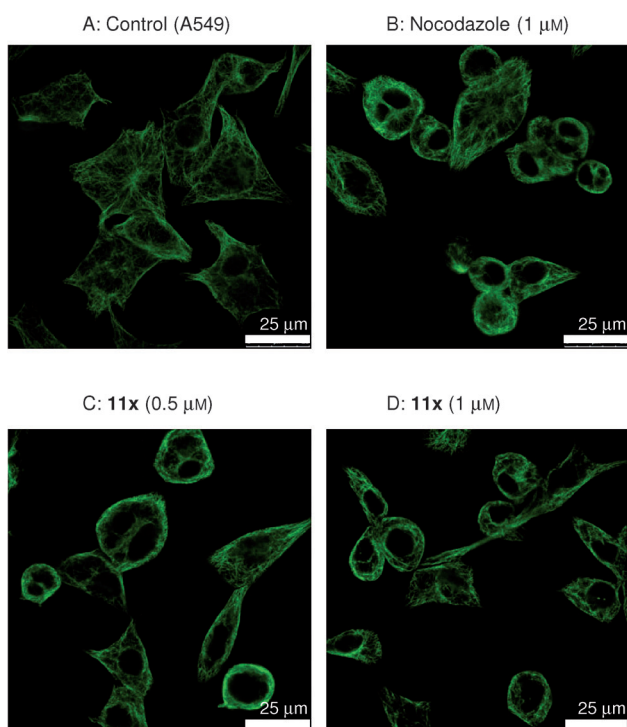


**Figure 5.** Immunohistochemistry analysis of the effects of conjugates on the microtubule network. A549 cells were treated with conjugate **11x** (0.5 and 1  $\mu\text{M}$ ) for 24 h followed by staining with an antitubulin antibody and FITC-conjugated secondary antibody. Nocodazole was used as a reference compound. Microtubule organization was clearly observed as tubulin-network-like structures in control cells and was found to be disrupted in cells treated with conjugate **11x**.

### Hoechst staining for the effect on apoptosis

Apoptosis is one of the major pathways of programmed cell death. Chromatin condensation, nuclear shrinking, and fragmented nuclei are some of the characteristics of apoptotic

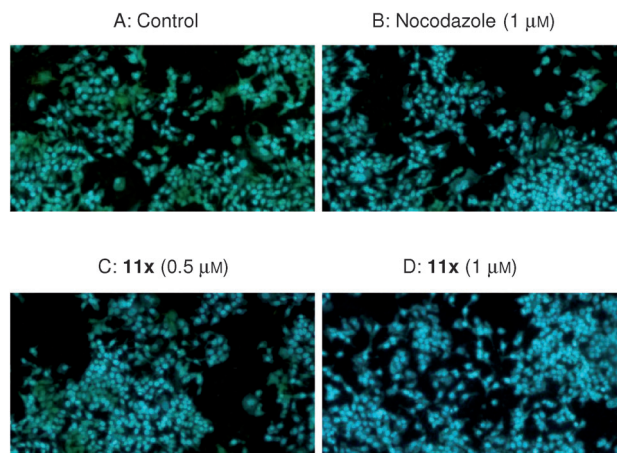


**Figure 6.** Hoechst staining in A549 lung cancer cell line. A: Control cells (A549), B: Nocodazole at 1  $\mu\text{M}$ , C: **11x** at 0.5  $\mu\text{M}$  and D: **11x** at 1  $\mu\text{M}$  concentration.

cells. Disruption of microtubule formation leads to cell-cycle arrest in the G2/M phase, followed by apoptotic cell death.<sup>[47]</sup> It was considered of interest to investigate the apoptosis-inducing effect of conjugate **11x** by Hoechst staining (H-33258) in A549 cells. Therefore, the cells were treated with nocodazole at 1  $\mu\text{M}$  and **11x** (0.5 and 1  $\mu\text{M}$ ) for 24 h. After treatment with these compounds, marked morphological changes, such as nuclear fragmentation, condensation of chromatin, and formation of apoptotic bodies, were observed as seen in Figure 6.

### Effect on caspase-3

From previous reports, it is well established that molecules affecting microtubule polymerization cause mitotic arrest and ultimately lead to apoptosis.<sup>[48]</sup> Caspases are a family of cysteine-aspartic proteases that are crucial mediators of apoptosis. Among them, caspase-3 is the best understood among the mammalian caspases in terms of its specificity and role in apoptosis. Caspase-3 is also required for some typical hallmarks of apoptosis.<sup>[49]</sup> There are a few reports<sup>[49–51]</sup> that indicate that cell-cycle arrest at the G2/M phase takes place by the induction of apoptosis. Hence, it was considered of interest to understand the correlation between the cytotoxicity of **11x** and the induction of apoptosis. A549 cells were treated with **11x** (0.5 and 1  $\mu\text{M}$ ) and examined for the activation of caspase-3 activity. Nocodazole was used as standard compound. Results indicate about a 2.5-fold induction in caspase-3 levels compared with the untreated control (Figure 7).

### Studying the apoptotic effect by Annexin V-FITC

The caspase-3 activity assay and Hoechst staining results suggest that this conjugate induces apoptosis in human lung cancer cell line A549. The apoptotic effect of **11x** was further evaluated by using a Annexin V-FITC/propidium iodide (AV/PI) dual staining assay<sup>[52]</sup> to examine the occurrence of phosphatidylserine externalization and also to understand whether it is due to physiological apoptosis or nonspecific necrosis. Noco-

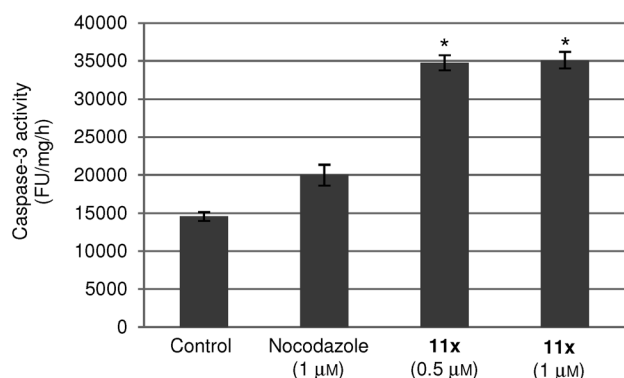


**Figure 7.** Effect of conjugate **11 x** on caspase-3 activity: A549 cells were treated with conjugate **11 x** (0.5 and 1 μM) for 24 h. Values indicated are the mean ± SD of two different experiments performed in triplicates. Statistical analysis was performed using GraphPad Prism software version 5.01. (\* $p < 0.05$  vs. control).

dazole was used as a reference compound. A549 cells were treated with nocodazole (1 μM) or conjugate **11 x** (0.5 and 1 μM) for 24 h to examine the apoptotic effect. After treatment, it was observed that conjugate **11 x** significantly induced apoptosis in A549 cells as shown in Figure 8. Results indicate

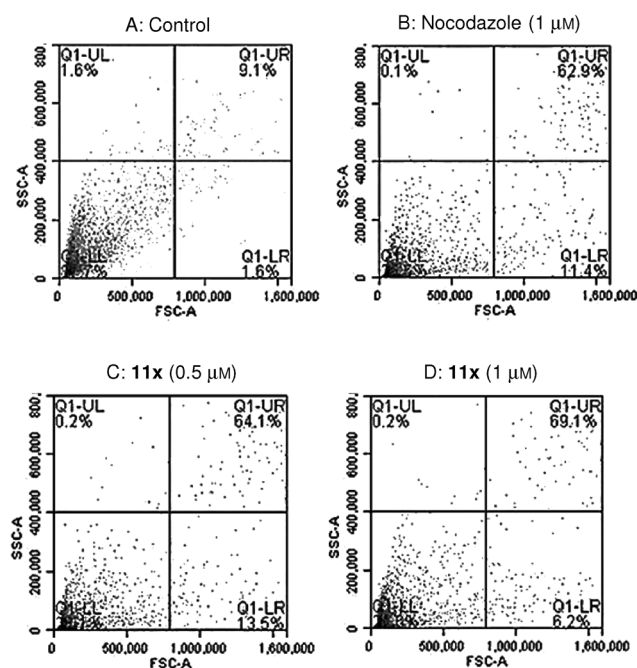


**Figure 8.** Annexin V-FITC staining results. A549 cells were treated with nocodazole and conjugate **11 x** (0.5 and 1 μM) for 24 h.

that this conjugate induces 64.14 and 69.07% apoptosis at 0.5 and 1 μM, respectively, and nocodazole caused 62.90% of cells to become apoptotic at 1 μM; in the untreated control, only 9.1% of cells were undergoing apoptosis (Table 3).

Sample	Upper left [%]	Upper Right <sup>[b]</sup> [%]	Lower left [%]	Lower right [%]
A: Control	1.64	9.10	87.70	1.56
B: Nocodazole (1 μM)	0.11	62.90	25.61	11.38
C: <b>11 x</b> (0.5 μM)	0.21	64.14	22.13	13.52
D: <b>11 x</b> (1 μM)	0.17	69.07	24.59	6.17

[a] Determined by Annexin V-FITC assay; data are the quantification of the FACS results shown in Figure 8. [b] Represent the percentage of cells undergoing apoptosis.

### DNA fragmentation analysis

Apoptosis is characterized by distinct morphologic changes, including cell shrinkage, membrane blebbing, chromatin condensation, DNA fragmentation, and the formation of apoptotic bodies.<sup>[53]</sup> During apoptosis DNA is cleaved into small fragments, and fragmented DNA produces a series of bands that are described as DNA ladders. These fragments can be observed by gel electrophoresis. In this context, A549 cells were treated with nocodazole (1 μM) or conjugate **11 x** (0.5 and 1 μM) for 24 h, and DNA was isolated from these cells. The DNA was run on 2% agarose gel electrophoresis, and staining was done with ethidium bromide under UV illumination. It was observed that **11 x** produces significant DNA fragmentation, which further indicates apoptosis (Figure 9).

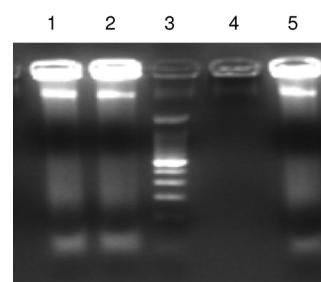


**Figure 9.** DNA fragmentation induced by conjugate **11 x** in A-549 lung cancer cells. Lane 1: **11 x** (0.5 μM), lane 2: **11 x** (1 μM), lane 3: marker (100 bp), lane 4: untreated control DNA, and lane-5: nocodazole (1 μM).

### Western blot analysis of Bcl-2 and Bax proteins

The members of the Bcl-2 family play a pivotal role in the regulation of the mitochondrial apoptotic pathway. Among these, Bcl-2 inhibits apoptosis, whereas Bax counterbalances the Bcl-2 effect and stimulates apoptosis.<sup>[54]</sup> In this context, A549 cells were treated with **11 x** (0.5 and 1 μM). After 48 h of treatment, it was observed that antiapoptotic Bcl-2 was downregulated and proapoptotic Bax was upregulated (Figure 10). These data reveal that the induction of apoptosis by these new conjugates is associated with Bcl-2 downregulation.

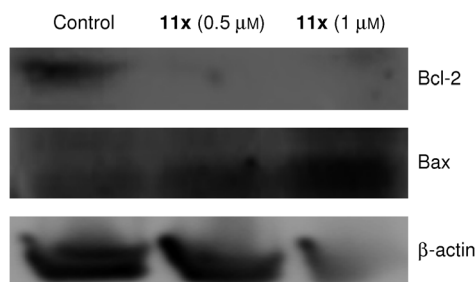


**Figure 10.** The effect of conjugates on Bcl-2 and Bax levels. A549 cells were treated with conjugate **11x** (0.5 and 1  $\mu\text{M}$ ) for 48 h. Cell lysates were collected, and the expression levels of Bcl-2 and Bax were determined by Western blot analysis.  $\beta$ -Actin was used as a loading control.

### Molecular docking studies

Molecular docking studies were performed by using AutoDock 4.2 to elucidate the interaction of this class of conjugates with tubulin and to investigate the binding mode of **11x**, **11i**, **11v**, and **11w** at the colchicine binding domain in the tubulin dimer. From the results of the modeling studies, conjugate **11x** is predicted to occupy the binding site of colchicine at the  $\alpha,\beta$ -interface of the tubulin with an orientation similar to that of the cocrystallized ligand. This observation supports the potent ability—similar to that of CA-4—shown by some of these conjugates to disrupt the microtubule assembly by inhibiting tubulin polymerization.

These conjugates were designed based on the CA-4 scaffold with the replacement of the olefinic linker by an imidazo-thiazolyl group. Compared with CA-4, molecular modelling suggests that these modifications result in improved binding interactions with the colchicine binding domain in the tubulin dimer. The 3,4,5-trimethoxyphenyl group in conjugate **11i** and 3,4-dimethoxyphenyl group in conjugate **11v** are predicted to form hydrophobic interactions with  $\alpha\text{Gln}11$ ,  $\beta\text{Asn}101$ , and  $\beta\text{Asn}249$ . These resemble the interactions of the 3,4,5-trimethoxy group of colchicine in the hydrophobic cavity of tubulin.<sup>[65]</sup> The binding pose of **11x** suggested that the pyridin-2-yl group forms hydrophobic interactions with  $\alpha\text{Asn}101$ . In addition, the model also suggests that hydrogen bonding interactions form between the carbonyl group of prop-2-ene-1-one and  $\alpha\text{Asn}101$ , in the range of 2.6–2.8 Å (Figure 11).

Figures 11 and 12 illustrate that, according to the modelling results, hydrogen bonding interactions may also form between the S-atom of the imidazo-[2,1-*b*]thiazol-5-yl group and  $\beta\text{Lys}352$  and between the N-atom of the imidazo[2,1-*b*]thiazol-5-yl group and  $\alpha\text{Asn}101$ . The model also suggests that the conjugate is also involved in hydrophobic and polar interactions with  $\alpha\text{Ser}178$ ,  $\alpha\text{Thr}179$ , and  $\beta\text{Thr}353$  in the colchicine binding site of tubulin. In addition, the 4-methoxy groups in **11x**, **11v** and **11w** are mod-

elled to interact with the hydrophobic pocket ( $\beta\text{Ala}250$ ,  $\beta\text{Lys}352$ , and  $\alpha\text{Gln}11$ ). Furthermore, the F-atom of the 4-fluorophenyl group in **11x**, **11i**, **11v** and **11w** is suggested to interact with  $\beta\text{Asn}249$ , which correlates with the antitubulin activity of these conjugates. These results postulate that conjugate **11x**, **11i**, **11v** and **11w** could strongly bind to the colchicine binding site of tubulin.

### Conclusions

In the present study, we have synthesized 2,3-diaryl imidazo-[1,2-*b*]thiazole–chalcone conjugates and evaluated them for their anticancer activity. The majority of these compounds demonstrated significant antiproliferative activities against

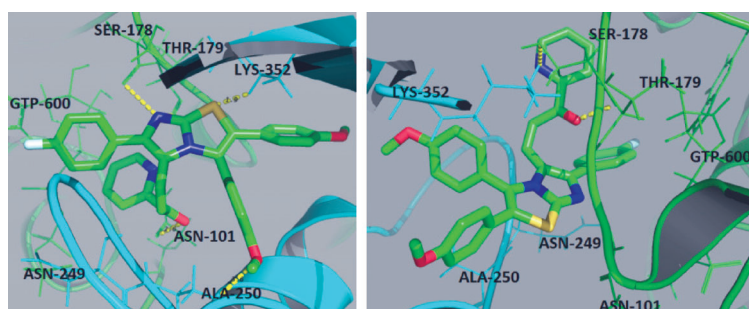


**Figure 11.** Representation of the binding pose of **11x** within the colchicine binding site. The orientation is similar to that of the cocrystallized colchicine fitted in the binding cavity at the  $\alpha,\beta$ -interface of the tubulin (PDB ID: 3E22<sup>[62]</sup>). Hydrophobic interactions are indicated by yellow dashed lines.

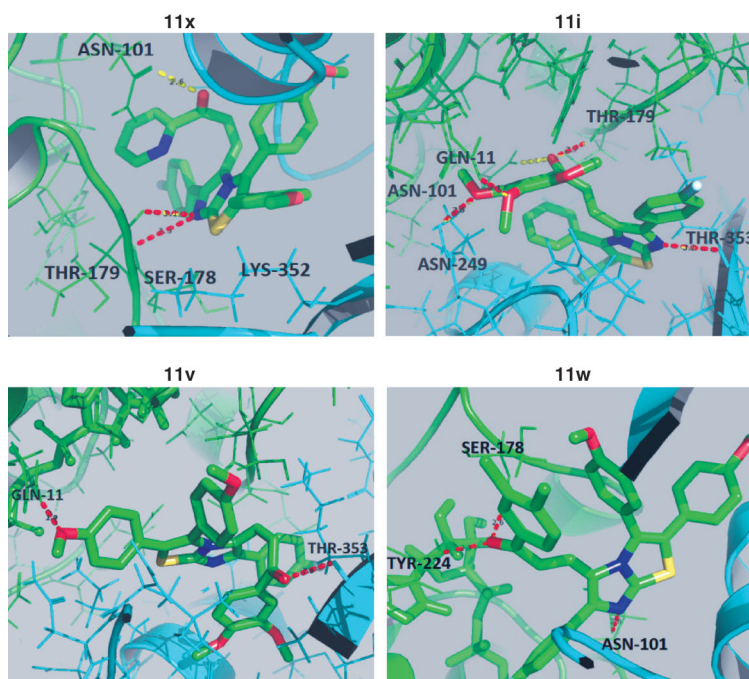


**Figure 12.** The predicted binding modes of conjugates **11x**, **11i**, **11v**, and **11w** (green stick model) within the colchicine binding site of tubulin (PDB ID: 3E22<sup>[62]</sup>). Surrounding amino acids are shown as chain A (green) and chain B (cyan) and are labelled in black. The hydrogen bonds are shown by red dashed lines, and the distance between the ligands and protein is less than 3 Å. Hydrophobic interactions are indicated by yellow dashed lines.

tested cancer cell lines. Among these conjugates, **11x**, which contains a pyridyl ring, is the most active. It showed potent anticancer efficacy against the human lung cancer A549 cell line with an  $IC_{50}$  value of 0.64  $\mu\text{M}$ . This conjugate also disrupted microtubule dynamics and induced abnormal spindle structure and centrosome formation, which resulted in cell-cycle arrest at the G2/M phase. Detailed biological studies, including Hoechst staining, a caspase-3 assay, DNA fragmentation analysis, and an Annexin V-FITC assay, confirm that this conjugate induces apoptosis. Moreover, docking experiments showed that **11x** interacts and binds efficiently with tubulin at the colchicine binding site. This was further confirmed using colchicine in a competition binding assay. Based on these results, conjugates containing both 2,3-diaryl imidazo[1,2-*b*]thiazole and chalcone moieties are effective tubulin polymerization inhibitors and could be further developed as potential anticancer agents.

## Experimental Section

### Chemistry

All chemicals and reagents were obtained from Aldrich (Sigma-Aldrich, St. Louis, MO, USA), Lancaster (Alfa Aesar, Johnson Matthey Company, Ward Hill, MA, USA), and Spectrochem Pvt. Ltd. (Mumbai, India) and were used without further purification unless indicated.  $\text{CH}_2\text{Cl}_2$  was distilled from  $\text{CaH}_2$  immediately prior to use. Reactions were monitored by thin-layer chromatography (TLC) performed on silica gel glass plates containing 60 GF-254, and visualization was achieved by UV light and iodine indicator, as well as by charring. Column chromatography was performed with Merck 60–120 mesh silica gel.  $^1\text{H}$  NMR spectra were recorded on Bruker UXNMR/XWIN (300 MHz) or Inova Varian VXR Unity (400, 500 MHz) NMR instrument. Chemical shifts ( $\delta$ ) are reported in parts per million (ppm) downfield from an internal tetramethylsilane (TMS) standard. FT-IR spectra for all compounds were recorded using thin film as well as a KBr disk. electrospray ionisation mass spectrometry (ESI-MS) was performed on a Micromass Quattro LC using ESI+ software with capillary voltage 3.98 kV and an ESI-mode-positive ion-trap detector. High-resolution mass spectra (HRMS) were recorded on a QSTAR XL Hybrid MS-MS mass spectrometer. Melting points were determined by means of an electrothermal melting point apparatus and are uncorrected.

### General procedures

**General reaction procedure for the preparation of compounds (5a,b):** Appropriate compound **4** (1 equiv) was dissolved in  $\text{CH}_2\text{Cl}_2$  (70 mL),  $\text{SOCl}_2$  (4 equiv), and 3 or 4 drops of DMF were added at  $0^\circ\text{C}$  under a nitrogen atmosphere, and the reaction was stirred for 1 h at  $0^\circ\text{C}$ . After completion of reaction,  $\text{CH}_2\text{Cl}_2$  and excess  $\text{SOCl}_2$  were removed in vacuo. Water (80 mL) and EtOAc (150 mL) were added to the residue, and the EtOAc layer was separated, dried with  $\text{Na}_2\text{SO}_4$ , filtered, and concentrated. Purification by column chromatography (EtOAc/petroleum ether, 1:19) gave desired compound **5**.

**2-Chloro-1,2-diphenylethanone (5a):** Pale yellow solid (5.38 g, 82%); mp: 75–78  $^\circ\text{C}$ ;  $^1\text{H}$  NMR (500 MHz,  $\text{CDCl}_3$ ):  $\delta$  = 7.95 (d,  $J$  = 7.17 Hz, 2H), 7.53 (d,  $J$  = 14.80, 7.32 Hz, 1H), 7.48 (d,  $J$  = 7.01 Hz, 2H), 7.42 (t,  $J$  = 7.78 Hz, 2H), 7.39–7.31 (m, 3H), 6.32 ppm (s, 1H); MS (ESI):  $m/z$  253 [ $M + \text{Na}$ ] $^+$ .

**2-Chloro-1,2-bis(4-methoxyphenyl)ethanone (5b):** Pale yellow solid (5.45 g, 73%); mp: 120–124  $^\circ\text{C}$ ;  $^1\text{H}$  NMR (300 MHz,  $\text{CDCl}_3$ ):  $\delta$  = 7.94 (d,  $J$  = 8.8 Hz, 2H), 7.40 (d,  $J$  = 8.8 Hz, 2H), 6.87–6.91 (m, 4H), 6.29 (s, 1H), 3.84 (s, 3H), 3.79 ppm (s, 3H); MS (ESI):  $m/z$  291 [ $M + \text{H}$ ] $^+$ .

**General reaction procedure for the preparation of compounds (6a,b):** A mixture of the appropriate compound **5** (1 equiv) and thiourea (1.2 equiv) was stirred in EtOH (5 mL) at  $80^\circ\text{C}$  under vigorous magnetic stirring for 15 h. The progress of the reaction was monitored by TLC. After completion of the reaction, EtOH was evaporated, and the product was extracted using EtOAc (2  $\times$  215 mL). The combined organic layers were separated, dried over anhydrous  $\text{MgSO}_4$  and concentrated in vacuo to obtain the crude solid product. Purification by column chromatography (EtOAc/petroleum ether, 3:7) afforded the corresponding derivative **6**.

**4,5-Diphenylthiazol-2-amine (6a):** White solid (3.5 g, 67%); mp: 214–218  $^\circ\text{C}$ ;  $^1\text{H}$  NMR (300 MHz,  $\text{CDCl}_3$ ):  $\delta$  = 7.45 (s, 2H), 7.26 (s, 8H), 5.14 ppm (s, 2H);  $^{13}\text{C}$  NMR (75 MHz,  $\text{CDCl}_3 + [\text{D}_6]\text{DMSO}$ ):  $\delta$  = 166.12, 141.35, 132.79, 131.19, 128.41, 127.94, 127.89, 127.49, 127.16, 126.80, 119.44 ppm; MS (ESI):  $m/z$  253 [ $M + \text{H}$ ] $^+$ .

**4,5-Bis(4-methoxyphenyl)thiazol-2-amine (6b):** White solid (3.71 g, 64%); mp: 233–237  $^\circ\text{C}$ ;  $^1\text{H}$  NMR (300 MHz,  $\text{CDCl}_3$ ):  $\delta$  = 7.39 (d,  $J$  = 9.06 Hz, 2H), 7.21 (d,  $J$  = 9.06 Hz, 2H), 6.80 (dd,  $J$  = 9.06, 7.55 Hz, 4H), 5.02 (br s, 2H), 3.81 (s, 3H), 3.79 ppm (s, 3H);  $^{13}\text{C}$  NMR (75 MHz,  $\text{CDCl}_3 + [\text{D}_6]\text{DMSO}$ ):  $\delta$  = 164.43, 157.32, 143.01, 129.25, 128.62, 126.97, 124.16, 117.82, 112.78, 112.13, 53.95, 53.86 ppm; MS (ESI):  $m/z$  313 [ $M + \text{H}$ ] $^+$ .

**General reaction procedure for the preparation of compounds (8a–f):** A mixture of amino thiazole (**6a,b**; 1 equiv) and phenacyl bromide (**7a–c**; 2 equiv) in *i*PrOH (20 mL) was heated at reflux for 2 h. Water (20 mL) was added to the reaction, and the mixture was cooled. The precipitate was collected by filtration, washed with 90% *i*PrOH, and recrystallized from 80% 2-methoxyethanol/ $\text{H}_2\text{O}$  to yield the desired compound (**8a–f**).

**6-(4-Methoxyphenyl)-2,3-diphenylimidazo[2,1-*b*]thiazole (8a):** Off-white solid (810 mg, 56%); mp: 199–203  $^\circ\text{C}$ ;  $^1\text{H}$  NMR (300 MHz,  $\text{CDCl}_3$ ):  $\delta$  = 7.74 (d,  $J$  = 8.68 Hz, 2H), 7.52 (s, 1H), 7.48 (s, 5H), 7.28 (s, 5H), 6.92 (d,  $J$  = 8.68 Hz, 2H), 3.84 ppm (s, 3H);  $^{13}\text{C}$  NMR (125 MHz,  $\text{CDCl}_3$ ):  $\delta$  = 159.01, 147.44, 146.60, 131.60, 129.67, 129.55, 129.38, 129.30, 128.96, 128.71, 128.30, 126.85, 126.37, 125.37, 114.01, 106.10, 55.52 ppm; MS (ESI):  $m/z$  383 [ $M + \text{H}$ ] $^+$ .

**6-(4-Chlorophenyl)-2,3-diphenylimidazo[2,1-*b*]thiazole (8b):** White solid (840 mg, 60%); mp: 192–197  $^\circ\text{C}$ ;  $^1\text{H}$  NMR (300 MHz,  $\text{CDCl}_3$ ):  $\delta$  = 7.75 (d,  $J$  = 8.30 Hz, 2H), 7.60 (s, 1H), 7.48 (s, 5H), 7.35 (d,  $J$  = 9.06 Hz, 2H), 7.28 ppm (s, 5H);  $^{13}\text{C}$  NMR (75 MHz,  $\text{CDCl}_3$ ):  $\delta$  = 147.79, 145.64, 132.84, 132.62, 131.44, 129.67, 129.52, 129.37, 128.97, 128.74, 128.45, 126.83, 126.33, 125.95, 107.22 ppm; MS (ESI):  $m/z$  387 [ $M + \text{H}$ ] $^+$ .

**6-(4-Fluorophenyl)-2,3-diphenylimidazo[2,1-*b*]thiazole (8c):** White solid (900 mg, 57%); mp: 196–199  $^\circ\text{C}$ ;  $^1\text{H}$  NMR (300 MHz,  $\text{CDCl}_3$ ):  $\delta$  = 7.85 (dd,  $J$  = 9.06, 5.28 Hz, 2H), 7.64 (s, 1H), 7.61–7.50 (m, 5H), 7.44–7.27 (m, 5H), 7.14 (t,  $J$  = 9.06 Hz, 2H);  $^{13}\text{C}$  NMR (125 MHz,  $\text{CDCl}_3$ ):  $\delta$  = 163.28, 161.31, 148.00, 143.43, 131.92, 131.10, 129.93, 129.32, 129.26, 128.90, 128.61, 128.40, 128.30, 128.20, 127.08, 115.29, 115.12, 90.35 ppm; MS (ESI):  $m/z$  371 [ $M + \text{H}$ ] $^+$ .

**2,3,6-Tris(4-methoxyphenyl)imidazo[2,1-*b*]thiazole (8d):** Off-white solid (900 mg, 52%); mp: 255–259  $^\circ\text{C}$ ;  $^1\text{H}$  NMR (300 MHz,  $\text{CDCl}_3$ ):  $\delta$  = 7.74 (d,  $J$  = 9.06 Hz, 2H), 7.50 (s, 1H), 7.40 (d,  $J$  = 9.06 Hz, 2H), 7.21 (d,  $J$  = 9.06 Hz, 2H), 6.99 (d,  $J$  = 8.30 Hz, 2H), 6.92 (d,  $J$  =

8.30 Hz, 2H), 6.82 (d,  $J=9.06$  Hz, 2H), 3.88 (s, 3H), 3.84 (s, 3H), 3.80 ppm (s, 3H);  $^{13}\text{C}$  NMR (125 MHz,  $\text{CDCl}_3$ ):  $\delta=160.14, 159.38, 158.85, 147.06, 146.25, 130.64, 130.10, 126.95, 126.22, 125.91, 124.36, 123.99, 121.75, 114.62, 114.05, 113.91, 106.00, 55.23, 55.16$  ppm; MS (ESI):  $m/z$  443  $[M+H]^+$ .

**6-(4-Chlorophenyl)-2,3-bis(4-methoxyphenyl)imidazo[2,1-b]thiazole (8e)**: White solid (1.1 g, 58%); mp: 242–246 °C;  $^1\text{H}$  NMR (500 MHz,  $\text{CDCl}_3$ ):  $\delta=7.78$  (d,  $J=8.54$  Hz, 2H), 7.71 (s, 1H), 7.50 (d,  $J=8.85$  Hz, 2H), 7.35 (d,  $J=8.54$  Hz, 2H), 7.17 (d,  $J=8.85$  Hz, 2H), 7.07 (d,  $J=8.85$  Hz, 2H), 6.83 (d,  $J=8.69$  Hz, 2H), 3.90 (s, 3H), 3.82 ppm (s, 3H);  $^{13}\text{C}$  NMR (125 MHz,  $\text{CDCl}_3$ ):  $\delta=161.27, 160.63, 144.50, 136.78, 135.95, 131.10, 130.27, 129.47, 126.94, 126.87, 124.49, 120.92, 118.16, 115.44, 114.67, 108.44, 55.49, 55.32$  ppm; MS (ESI):  $m/z$  447  $[M+H]^+$ .

**6-(4-Fluorophenyl)-2,3-bis(4-methoxyphenyl)imidazo[2,1-b]thiazole (8f)**: White solid (834 mg, 55%); mp: 250–253 °C;  $^1\text{H}$  NMR (300 MHz,  $\text{CDCl}_3$ ):  $\delta=7.84$  (dd,  $J=9.06, 5.28$  Hz, 2H), 7.64 (s, 1H), 7.47 (d,  $J=8.30$  Hz, 2H), 7.19 (d,  $J=9.06$  Hz, 2H), 7.14 (d,  $J=9.06$  Hz, 2H), 7.07 (d,  $J=9.06$  Hz, 2H), 6.84 (d,  $J=9.06$  Hz, 2H), 3.91 (s, 3H), 3.82 ppm (s, 3H);  $^{13}\text{C}$  NMR (125 MHz,  $\text{CDCl}_3$ ):  $\delta=164.39, 162.38, 161.25, 160.63, 144.28, 136.78, 131.08, 130.25, 127.91, 126.94, 122.11, 120.82, 118.07, 116.57, 116.39, 115.41, 114.68, 108.02, 55.48, 55.31$  ppm; MS (ESI):  $m/z$  431  $[M+H]^+$ .

**General reaction procedure for the preparation of compounds (9a–f)**: Vilsmeier reagent was prepared at 0–5 °C by dropping  $\text{POCl}_3$  (10 equiv) into a stirred solution of DMF (10.5 equiv) in  $\text{CHCl}_3$  (10 mL). The appropriate compound **8** (1 equiv) in  $\text{CHCl}_3$  (20 mL) was added to the solution of Vilsmeier reagent whilst maintaining stirring and cooling at 0–5 °C. The reaction mixture was allowed to warm to RT for 3 h, and then heated at reflux for 10–12 h (according to a TLC test). The solvent was removed in vacuo, and the resulting oily liquid was poured onto ice. The corresponding aldehyde (**9a–f**) was collected by filtration, and recrystallized from EtOH (5 mL) to obtain the pure product.

**6-(4-Methoxyphenyl)-2,3-diphenylimidazo[2,1-b]thiazole-5-carbaldehyde (9a)**: White solid (696 mg, 86%); mp: 237–241 °C;  $^1\text{H}$  NMR (500 MHz,  $\text{CDCl}_3$ ):  $\delta=9.31$  (s, 1H), 7.87 (d,  $J=7.99$  Hz, 2H), 7.53–7.41 (m, 5H), 7.27 (d,  $J=7.99$  Hz, 3H), 7.21 (d,  $J=5.99$  Hz, 2H), 7.00 (d,  $J=8.99$  Hz, 2H), 3.87 ppm (s, 3H);  $^{13}\text{C}$  NMR (125 MHz,  $\text{CDCl}_3 + 1$  drop TFA- $d_1$ ):  $\delta=176.67, 162.06, 152.89, 150.56, 131.48, 130.68, 130.40, 130.21, 129.63, 129.33, 129.19, 129.06, 129.00, 128.37, 123.55, 119.93, 114.49, 55.43$  ppm; MS (ESI):  $m/z$  411  $[M+H]^+$ .

**6-(4-Chlorophenyl)-2,3-diphenylimidazo[2,1-b]thiazole-5-carbaldehyde (9b)**: White solid (680 mg, 80%); mp: 235–239 °C;  $^1\text{H}$  NMR (300 MHz,  $\text{CDCl}_3$ ):  $\delta=9.31$  (s, 1H), 7.88 (d,  $J=8.30$  Hz, 2H), 7.53–7.41 (m, 7H), 7.31–7.25 (m, 3H), 7.24–7.19 ppm (m, 2H); (75 MHz,  $\text{CDCl}_3 + 1$  drop TFA- $d_1$ ):  $\delta=176.73, 149.64, 138.36, 132.74, 131.23, 131.05, 130.18, 130.09, 129.77, 129.43, 129.19, 128.98, 128.46, 127.59, 124.90, 123.74$  ppm; MS (ESI):  $m/z$  415  $[M+H]^+$ .

**6-(4-Fluorophenyl)-2,3-diphenylimidazo[2,1-b]thiazole-5-carbaldehyde (9c)**: White solid (712 mg, 78%); mp: 240–243 °C;  $^1\text{H}$  NMR (300 MHz,  $\text{CDCl}_3$ ):  $\delta=9.31$  (s, 1H), 7.93 (dd,  $J=8.30, 5.28$  Hz, 2H), 7.55–7.41 (m, 5H), 7.31–7.11 ppm (m, 7H);  $^{13}\text{C}$  NMR (125 MHz,  $\text{CDCl}_3$ ):  $\delta=176.36, 161.95, 156.22, 153.19, 131.63, 131.52, 130.72, 130.19, 129.64, 129.21, 129.04, 128.83, 128.76, 128.52, 125.32, 115.53, 115.24$  ppm; MS (ESI):  $m/z$  399  $[M+H]^+$ .

**2,3,6-Tris(4-methoxyphenyl)imidazo[2,1-b]thiazole-5-carbaldehyde (9d)**: White solid (678 mg, 77%); mp: 260–264 °C;  $^1\text{H}$  NMR (300 MHz,  $\text{CDCl}_3$ ):  $\delta=9.35$  (s, 1H), 7.90 (d,  $J=8.68$  Hz, 2H), 7.35 (d,

$J=8.68$  Hz, 2H), 7.14 (d,  $J=8.68$  Hz, 2H), 6.98 (dd,  $J=8.68, 4.15$  Hz, 4H), 6.79 (d,  $J=8.68$  Hz, 2H), 3.87 (s, 6H), 3.78 ppm (s, 3H); (125 MHz,  $\text{CDCl}_3 + 1$  drop TFA- $d_1$ ):  $\delta=176.54, 160.65, 160.53, 159.67, 157.14, 152.86, 131.51, 131.01, 130.19, 129.29, 127.68, 125.36, 125.04, 123.21, 121.74, 114.54, 114.10, 113.66, 55.21$  ppm; MS (ESI):  $m/z$  471  $[M+H]^+$ .

**6-(4-Chlorophenyl)-2,3-bis(4-methoxyphenyl)imidazo[2,1-b]thiazole-5-carbaldehyde (9e)**: White solid (815 mg, 73%); mp: 267–269 °C;  $^1\text{H}$  NMR (500 MHz,  $\text{CDCl}_3$ ):  $\delta=9.32$  (s, 1H), 7.91 (d,  $J=8.99$  Hz, 2H), 7.42 (d,  $J=7.99$  Hz, 2H), 7.35 (d,  $J=7.99$  Hz, 2H), 7.14 (d,  $J=8.99$  Hz, 2H), 6.99 (d,  $J=8.99$  Hz, 2H), 6.79 (d,  $J=8.99$  Hz, 2H), 3.87 (s, 3H), 3.78 ppm (s, 3H); (125 MHz,  $\text{CDCl}_3 + 1$  drop TFA- $d_1$ ):  $\delta=176.83, 161.23, 160.37, 151.61, 150.60, 137.13, 131.61, 131.05, 130.24, 128.98, 127.44, 124.32, 121.67, 120.16, 115.18, 114.45, 55.32$  ppm; MS (ESI):  $m/z$  475  $[M+H]^+$ .

**6-(4-Fluorophenyl)-2,3-bis(4-methoxyphenyl)imidazo[2,1-b]thiazole-5-carbaldehyde (9f)**: White solid (720 mg, 81%); mp: 265–268 °C;  $^1\text{H}$  NMR (300 MHz,  $\text{CDCl}_3$ ):  $\delta=9.32$  (s, 1H), 7.95 (dd,  $J=8.30, 5.28$  Hz, 2H), 7.36 (d,  $J=8.30$  Hz, 2H), 7.18–7.11 (m, 4H), 6.99 (d,  $J=8.30$  Hz, 2H), 6.80 (d,  $J=9.06$  Hz, 2H), 3.88 (s, 3H), 3.79 ppm (s, 3H);  $^{13}\text{C}$  NMR (125 MHz,  $\text{CDCl}_3$ ):  $\delta=176.49, 164.50, 162.52, 160.73, 159.81, 155.52, 152.60, 131.55, 130.20, 129.08, 128.23, 125.38, 123.07, 121.49, 115.30, 115.14, 114.82, 114.19, 55.26$  ppm; MS (ESI):  $m/z$  459  $[M+H]^+$ .

**General procedure for the synthesis of chalcones (11a–x)**: A mixture of the corresponding acetophenone (1 equiv) and aldehyde (**9a–f**; 1 equiv) in anhydrous EtOH (3 mL for 1 mmol of acetophenone) was stirred at RT for 5 min. Then KOH (3 equiv) was added. The reaction mixture was stirred at 80 °C until the aldehyde was consumed (usually 6–12 h). After that, 10% aq HCl (approx. 80 mL) was added until pH 5 was obtained. In the case of the chalcones that precipitated, these were filtered and recrystallized from MeOH. In the other cases, the product was purified by using silica gel chromatography (EtOAc/petroleum ether, 7:13).

**(E)-3-(6-(4-Methoxyphenyl)-2,3-diphenylimidazo[2,1-b]thiazol-5-yl)-1-(3,4,5-trimethoxyphenyl)prop-2-en-1-one (11a)**: Yellow solid (167 mg, 76%); mp: 213–216 °C; FT-IR:  $\tilde{\nu}=2967, 2937, 2837, 1650, 1572, 1019, 697$   $\text{cm}^{-1}$ ;  $^1\text{H}$  NMR (300 MHz,  $\text{CDCl}_3$ ):  $\delta=7.65$  (d,  $J=8.30$  Hz, 2H), 7.58–7.45 (m, 4H), 7.29–7.20 (m, 7H), 7.00 (d,  $J=8.30$  Hz, 2H), 6.82 (s, 2H), 6.79 (d,  $J=15.86$  Hz, 1H), 3.87 (s, 3H), 3.85 (s, 3H), 3.78 ppm (s, 6H);  $^{13}\text{C}$  NMR (75 MHz,  $\text{CDCl}_3$ ):  $\delta=187.35, 159.74, 152.73, 150.28, 141.73, 133.26, 131.05, 130.50, 130.44, 130.38, 129.63, 129.48, 129.04, 128.81, 128.70, 128.60, 128.44, 128.35, 128.15, 127.53, 121.74, 118.28, 114.04, 105.27, 60.80, 56.06, 55.15$  ppm; MS (ESI):  $m/z$  603  $[M+H]^+$ ; HRMS (ESI):  $m/z$   $[M+H]^+$  calcd for  $\text{C}_{36}\text{H}_{31}\text{N}_2\text{O}_5\text{S}$ : 603.1948, found: 603.1949.

**(E)-1-(3,4-Dimethoxyphenyl)-3-(6-(4-methoxyphenyl)-2,3-diphenylimidazo[2,1-b]thiazol-5-yl)prop-2-en-1-one (11b)**: Yellow solid (148 mg, 71%); mp: 206–209 °C; FT-IR:  $\tilde{\nu}=2956, 2919, 2849, 1650, 1596, 1452, 1022, 702$   $\text{cm}^{-1}$ ;  $^1\text{H}$  NMR (300 MHz,  $\text{CDCl}_3$ ):  $\delta=7.67$  (d,  $J=9.06$  Hz, 2H), 7.54–7.45 (m, 5H), 7.34–7.17 (m, 7H), 7.07–7.02 (dd,  $J=8.30, 2.26$  Hz, 1H), 7.01–6.98 (d,  $J=9.06$  Hz, 2H), 6.74 (d,  $J=8.30$  Hz, 1H), 6.69 (d,  $J=15.10$  Hz, 1H), 3.91 (s, 3H), 3.86 (s, 3H), 3.85 ppm (s, 3H);  $^{13}\text{C}$  NMR (75 MHz,  $\text{CDCl}_3$ ):  $\delta=187.14, 159.75, 152.67, 150.49, 150.25, 148.71, 131.17, 131.05, 130.62, 130.32, 129.34, 129.25, 129.19, 129.10, 128.90, 128.84, 128.57, 128.41, 128.09, 126.95, 122.41, 121.66, 119.12, 114.04, 110.34, 109.61, 55.91, 55.82, 55.24$  ppm; MS (ESI):  $m/z$  573  $[M+H]^+$ ; HRMS (ESI):  $m/z$   $[M+H]^+$  calcd for  $\text{C}_{35}\text{H}_{29}\text{N}_2\text{O}_4\text{S}$ : 573.1842, found: 573.1838.

**(E)-1-(3,4-Dichlorophenyl)-3-(6-(4-methoxyphenyl)-2,3-diphenylimidazo[2,1-b]thiazol-5-yl)prop-2-en-1-one (11 c):** Yellow solid (165 mg, 78%); mp: 201–205 °C; FT-IR:  $\tilde{\nu}$  = 2970, 2850, 1655, 1606, 1585, 1228, 1026, 695  $\text{cm}^{-1}$ ;  $^1\text{H NMR}$  (300 MHz,  $\text{CDCl}_3$ ):  $\delta$  = 7.65 (d,  $J$  = 9.06 Hz, 2H), 7.51 (d,  $J$  = 2.26 Hz, 1H), 7.47 (m, 4H), 7.43–7.34 (m, 3H), 7.30–7.25 (m, 4H), 7.24–7.18 (m, 2H), 7.03 (d,  $J$  = 8.30 Hz, 2H), 6.34 (d,  $J$  = 15.86 Hz, 1H), 3.88 ppm (s, 3H);  $^{13}\text{C NMR}$  (125 MHz,  $\text{CDCl}_3$ ):  $\delta$  = 186.88, 160.12, 152.31, 151.63, 137.71, 136.52, 132.64, 131.18, 131.06, 130.68, 130.47, 130.37, 130.35, 130.04, 129.41, 129.20, 129.04, 128.98, 128.71, 128.60, 127.45, 127.14, 126.89, 121.48, 117.88, 114.25, 55.35 ppm; MS (ESI):  $m/z$  581  $[M+H]^+$ ; HRMS (ESI):  $m/z$   $[M+H]^+$  calcd for  $\text{C}_{33}\text{H}_{23}\text{Cl}_2\text{N}_2\text{O}_2\text{S}$ : 581.0851, found: 581.0850.

**(E)-3-(6-(4-Methoxyphenyl)-2,3-diphenylimidazo[2,1-b]thiazol-5-yl)-1-(pyridin-2-yl)prop-2-en-1-one (11 d):** Yellow solid (118 mg, 63%); mp: 193–197 °C; FT-IR:  $\tilde{\nu}$  = 2969, 2856, 1665, 1609, 1589, 1055, 694  $\text{cm}^{-1}$ ;  $^1\text{H NMR}$  (300 MHz,  $\text{CDCl}_3$ ):  $\delta$  = 8.49 (d,  $J$  = 4.53 Hz, 1H), 7.91 (d,  $J$  = 8.30 Hz, 1H), 7.76–7.66 (m, 3H), 7.48–7.31 (m, 7H), 7.27–7.18 (m, 6H), 6.98 (d,  $J$  = 8.30 Hz, 2H), 3.85 ppm (s, 3H);  $^{13}\text{C NMR}$  (125 MHz,  $\text{CDCl}_3$ ):  $\tilde{\nu}$  = 188.84, 159.76, 154.18, 151.04, 150.92, 148.44, 136.48, 131.26, 130.65, 130.09, 130.02, 129.38, 129.18, 129.08, 128.98, 128.90, 128.58, 128.38, 127.02, 126.82, 126.15, 122.34, 121.93, 119.53, 114.02, 55.27 ppm; MS (ESI):  $m/z$  514  $[M+H]^+$ ; HRMS (ESI):  $m/z$   $[M+H]^+$  calcd for  $\text{C}_{32}\text{H}_{24}\text{N}_3\text{O}_2\text{S}$ : 514.1583, found: 514.1578.

**(E)-3-(6-(4-Chlorophenyl)-2,3-diphenylimidazo[2,1-b]thiazol-5-yl)-1-(3,4,5-trimethoxyphenyl)prop-2-en-1-one (11 e):** Yellow solid (158 mg, 72%); mp: 213–216 °C; FT-IR:  $\tilde{\nu}$  = 2997, 2937, 2835, 1650, 1569, 1124, 732  $\text{cm}^{-1}$ ;  $^1\text{H NMR}$  (300 MHz,  $\text{CDCl}_3$ ):  $\delta$  = 7.68 (d,  $J$  = 8.30 Hz, 2H), 7.58–7.42 (m, 7H), 7.30–7.23 (m, 5H), 7.20 (d,  $J$  = 15.11 Hz, 1H), 6.82 (s, 2H), 6.78 (d,  $J$  = 15.11 Hz, 1H), 3.88 (s, 3H), 3.80 ppm (s, 6H);  $^{13}\text{C NMR}$  (75 MHz,  $\text{CDCl}_3$ ):  $\delta$  = 187.05, 152.81, 150.52, 148.54, 141.93, 134.34, 133.73, 133.03, 130.94, 130.49, 129.57, 129.37, 129.27, 129.16, 128.99, 128.90, 128.84, 128.70, 128.58, 128.38, 127.59, 122.03, 119.30, 105.28, 60.83, 56.08 ppm; MS (ESI):  $m/z$  607  $[M+H]^+$ ; HRMS (ESI):  $m/z$   $[M+H]^+$  calcd for  $\text{C}_{35}\text{H}_{28}\text{ClN}_2\text{O}_4\text{S}$ : 607.1452, found: 607.1456.

**(E)-3-(6-(4-Chlorophenyl)-2,3-diphenylimidazo[2,1-b]thiazol-5-yl)-1-(3,4-dimethoxyphenyl)prop-2-en-1-one (11 f):** Yellow solid (135 mg, 65%); mp: 210–214 °C; FT-IR:  $\tilde{\nu}$  = 2912, 2850, 1651, 1265, 1021, 761  $\text{cm}^{-1}$ ;  $^1\text{H NMR}$  (300 MHz,  $\text{CDCl}_3$ ):  $\delta$  = 7.68 (d,  $J$  = 8.49 Hz, 1H), 7.54–7.41 (m, 5H), 7.36–7.31 (m, 1H), 7.30–7.20 (m, 7H), 7.03 (dd,  $J$  = 8.68, 1.88 Hz, 1H), 6.77 (d,  $J$  = 8.49 Hz, 1H), 6.68 (d,  $J$  = 15.67 Hz, 1H), 6.46 (q,  $J$  = 24.5, 11.7 Hz, 1H), 3.92 (s, 3H), 3.85 ppm (d,  $J$  = 5.85 Hz, 1H);  $^{13}\text{C NMR}$  (75 MHz,  $\text{CDCl}_3$ ):  $\delta$  = 186.88, 152.84, 150.49, 148.80, 148.51, 134.23, 133.41, 131.20, 131.00, 130.82, 130.62, 130.39, 129.40, 129.11, 128.99, 128.84, 128.73, 128.64, 128.52, 128.29, 128.17, 122.47, 122.04, 120.29, 110.28, 109.70, 55.94, 55.82 ppm; MS (ESI):  $m/z$  577  $[M+H]^+$ ; HRMS (ESI):  $m/z$   $[M+H]^+$  calcd for  $\text{C}_{34}\text{H}_{26}\text{ClN}_2\text{O}_3\text{S}$ : 577.1347, found: 577.1345.

**(E)-3-(6-(4-Chlorophenyl)-2,3-diphenylimidazo[2,1-b]thiazol-5-yl)-1-(3,4-dichlorophenyl)prop-2-en-1-one (11 g):** Yellow solid (146 mg, 69%); mp: 209–213 °C; FT-IR:  $\tilde{\nu}$  = 3049, 1653, 1584, 1013, 852, 705;  $^1\text{H NMR}$  (300 MHz,  $\text{CDCl}_3$ ):  $\delta$  = 7.66 (d,  $J$  = 8.49 Hz, 2H), 7.50–7.41 (m, 5H), 7.39–7.31 (m, 3H), 7.30–7.19 (m, 7H), 6.41–6.21 ppm (m, 2H);  $^{13}\text{C NMR}$  (75 MHz,  $\text{CDCl}_3$ ):  $\delta$  = 186.74, 151.62, 150.55, 137.45, 136.77, 134.81, 132.99, 132.78, 131.19, 130.91, 130.68, 130.41, 130.06, 129.70, 129.41, 129.04, 128.74, 128.59, 128.44, 127.93, 127.10, 121.77, 119.16 ppm; MS (ESI):  $m/z$  585  $[M+H]^+$ ; HRMS (ESI):  $m/z$   $[M+H]^+$  calcd for  $\text{C}_{32}\text{H}_{20}\text{Cl}_3\text{N}_2\text{O}_2\text{S}$ : 585.0353, found: 585.0356.

**(E)-3-(6-(4-Chlorophenyl)-2,3-diphenylimidazo[2,1-b]thiazol-5-yl)-1-(pyridin-2-yl)prop-2-en-1-one (11 h):** Yellow solid (108 mg, 58%); mp: 189–194 °C; FT-IR:  $\tilde{\nu}$  = 2918, 1667, 1597, 1282, 1012, 837, 692  $\text{cm}^{-1}$ ;  $^1\text{H NMR}$  (500 MHz,  $\text{CDCl}_3$ ):  $\delta$  = 8.51 (d,  $J$  = 4.73 Hz, 1H), 7.92 (d,  $J$  = 7.78 Hz, 1H), 7.74 (dt,  $J$  = 7.62, 1.83 Hz, 1H), 7.70 (d,  $J$  = 8.54 Hz, 2H), 7.45–7.42 (m, 4H), 7.40 (d,  $J$  = 8.54 Hz, 2H), 7.37–7.29 (m, 3H), 7.25–7.18 ppm (m, 6H);  $^{13}\text{C NMR}$  (125 MHz,  $\text{CDCl}_3$ ):  $\delta$  = 188.69, 153.93, 150.78, 149.13, 148.58, 136.58, 134.21, 133.12, 131.11, 130.66, 130.24, 130.17, 129.51, 129.24, 128.96, 128.81, 128.73, 128.65, 128.52, 128.45, 127.33, 126.37, 122.40, 122.34, 120.60 ppm; MS (ESI):  $m/z$  518  $[M+H]^+$ ; HRMS (ESI):  $m/z$   $[M+H]^+$  calcd for  $\text{C}_{31}\text{H}_{21}\text{ClN}_3\text{O}_2\text{S}$ : 518.1088, found: 518.1082.

**(E)-3-(6-(4-Fluorophenyl)-2,3-diphenylimidazo[2,1-b]thiazol-5-yl)-1-(3,4,5-trimethoxyphenyl)prop-2-en-1-one (11 i):** Yellow solid (162 mg, 73%); mp: 210–213 °C; FT-IR:  $\tilde{\nu}$  = 2936, 1651, 1574, 1126, 697  $\text{cm}^{-1}$ ;  $^1\text{H NMR}$  (300 MHz,  $\text{CDCl}_3$ ):  $\delta$  = 7.70 (dd,  $J$  = 8.68, 5.47 Hz, 2H), 7.58–7.44 (m, 5H), 7.30–7.21 (m, 5H), 7.17 (q,  $J$  = 8.68, 4.53 Hz, 3H), 6.80 (s, 2H), 6.70 (d,  $J$  = 15.48 Hz, 1H), 3.87 (s, 3H), 3.79 ppm (s, 6H);  $^{13}\text{C NMR}$  (75 MHz,  $\text{CDCl}_3$ ):  $\delta$  = 187.20, 152.82, 150.49, 149.00, 142.00, 133.10, 131.36, 131.08, 131.02, 130.55, 130.50, 129.56, 129.39, 129.03, 128.89, 128.59, 128.54, 128.34, 127.51, 121.99, 119.10, 115.83, 115.65, 105.36, 60.85, 56.11 ppm; MS (ESI):  $m/z$  591  $[M+H]^+$ ; HRMS (ESI):  $m/z$   $[M+H]^+$  calcd for  $\text{C}_{35}\text{H}_{28}\text{FN}_2\text{O}_4\text{S}$ : 591.1748, found: 591.1747.

**(E)-1-(3,4-Dimethoxyphenyl)-3-(6-(4-fluorophenyl)-2,3-diphenylimidazo[2,1-b]thiazol-5-yl)prop-2-en-1-one (11 j):** Yellow solid (156 mg, 74%); mp: 210–214 °C; FT-IR:  $\tilde{\nu}$  = 2921, 1644, 1567, 1267, 1023, 750  $\text{cm}^{-1}$ ;  $^1\text{H NMR}$  (300 MHz,  $\text{CDCl}_3$ ):  $\delta$  = 7.72 (dd,  $J$  = 9.06, 5.28 Hz, 2H), 7.55–7.45 (m, 5H), 7.31–7.22 (m, 7H), 7.17 (t,  $J$  = 8.30 Hz, 2H), 7.03 (dd,  $J$  = 9.06, 2.26 Hz, 1H), 6.76 (d,  $J$  = 9.06 Hz, 1H), 6.68 (d,  $J$  = 15.86 Hz, 1H), 3.92 (s, 3H), 3.86 ppm (s, 3H);  $^{13}\text{C NMR}$  (125 MHz,  $\text{CDCl}_3$ ):  $\delta$  = 186.91, 163.71, 161.74, 152.83, 150.44, 148.94, 148.81, 131.05, 130.91, 130.85, 130.62, 130.38, 129.41, 128.90, 128.82, 128.71, 128.64, 128.51, 127.32, 122.40, 121.93, 119.82, 115.76, 115.59, 110.30, 109.66, 55.95, 55.84 ppm; MS (ESI):  $m/z$  561  $[M+H]^+$ ; HRMS (ESI):  $m/z$   $[M+H]^+$  calcd for  $\text{C}_{34}\text{H}_{26}\text{FN}_2\text{O}_3\text{S}$ : 561.1642, found: 561.1638.

**(E)-1-(3,4-Dichlorophenyl)-3-(6-(4-fluorophenyl)-2,3-diphenylimidazo[2,1-b]thiazol-5-yl)prop-2-en-1-one (11 k):** Yellow solid (169 mg, 79%); mp: 194–198 °C; FT-IR:  $\tilde{\nu}$  = 2920, 1653, 1573, 1219, 1026, 695  $\text{cm}^{-1}$ ;  $^1\text{H NMR}$  (300 MHz,  $\text{CDCl}_3$ ):  $\delta$  = 6.79 (q,  $J$  = 8.68, 5.47 Hz, 2H), 7.52–7.42 (m, 6H), 7.39 (d,  $J$  = 6.61 Hz, 1H), 7.35–7.31 (m, 2H), 7.30–7.24 (m, 3H), 7.23–7.17 (m, 4H), 6.28 ppm (d,  $J$  = 15.48 Hz, 1H);  $^{13}\text{C NMR}$  (75 MHz,  $\text{CDCl}_3$ ):  $\delta$  = 186.71, 164.60, 161.28, 137.40, 132.68, 130.99, 130.88, 130.71, 130.62, 130.56, 130.50, 130.39, 129.98, 129.37, 129.19, 129.05, 129.01, 128.76, 128.67, 128.55, 128.46, 127.01, 121.60, 118.63, 115.99, 115.69 ppm; MS (ESI):  $m/z$  569  $[M+H]^+$ ; HRMS (ESI):  $m/z$   $[M+H]^+$  calcd for  $\text{C}_{32}\text{H}_{20}\text{Cl}_2\text{FN}_2\text{O}_2\text{S}$ : 569.065, found: 569.0650.

**(E)-3-(6-(4-Fluorophenyl)-2,3-diphenylimidazo[2,1-b]thiazol-5-yl)-1-(pyridin-2-yl)prop-2-en-1-one (11 l):** Yellow solid (113 mg, 60%); mp: 188–192 °C; FT-IR:  $\tilde{\nu}$  = 1671, 1594, 1278, 742  $\text{cm}^{-1}$ ;  $^1\text{H NMR}$  (500 MHz,  $\text{CDCl}_3$ ):  $\delta$  = 8.50 (d,  $J$  = 3.81 Hz, 1H), 7.91 (d,  $J$  = 7.78 Hz, 1H), 7.76–7.67 (m, 3H), 7.47–7.41 (m, 5H), 7.39–7.32 (m, 2H), 7.31–7.18 (m, 6H), 7.13 ppm (t,  $J$  = 8.69 Hz, 2H);  $^{13}\text{C NMR}$  (75 MHz,  $\text{CDCl}_3$ ):  $\delta$  = 188.69, 164.39, 161.11, 153.92, 149.56, 148.50, 136.52, 131.17, 131.08, 130.82, 130.74, 130.62, 130.12, 129.60, 129.25, 128.90, 128.70, 128.61, 128.47, 128.08, 126.31, 122.35, 119.97, 115.69, 115.40 ppm; MS (ESI):  $m/z$  502  $[M+H]^+$ ; HRMS (ESI):  $m/z$   $[M+H]^+$  calcd for  $\text{C}_{31}\text{H}_{21}\text{FN}_3\text{O}_2\text{S}$ : 502.1383, found: 502.1374.

**(E)-1-(3,4,5-Trimethoxyphenyl)-3-(2,3,6-tris(4-methoxyphenyl)-imidazo[2,1-b]thiazol-5-yl)prop-2-en-1-one (11 m):** Yellow solid (171 mg, 81%); mp: 194–199 °C; FT-IR:  $\tilde{\nu}$  = 2926, 1651, 1586, 1124, 834;  $^1\text{H NMR}$  (300 MHz,  $\text{CDCl}_3$ ):  $\delta$  = 7.64 (d,  $J$  = 8.68 Hz, 2H), 7.42–7.25 (m, 3H), 7.18–7.05 (m, 3H), 7.02–6.94 (m, 2H), 6.83 (s, 2H), 6.81–6.60 (m, 4H), 3.93–3.71 ppm (m, 18H);  $^{13}\text{C NMR}$  (75 MHz,  $\text{CDCl}_3$ ):  $\delta$  = 187.55, 160.79, 159.68, 159.51, 152.70, 150.40, 150.34, 141.67, 133.38, 131.95, 130.41, 130.30, 129.77, 129.43, 128.47, 128.32, 127.51, 123.52, 121.66, 120.64, 118.69, 114.79, 114.03, 105.34, 60.77, 56.08, 55.15 ppm; MS (ESI):  $m/z$  663  $[M+H]^+$ ; HRMS (ESI):  $m/z$   $[M+H]^+$  calcd for  $\text{C}_{38}\text{H}_{35}\text{N}_2\text{O}_7\text{S}$ : 663.2159, found: 663.2162.

**(E)-1-(3,4-Dimethoxyphenyl)-3-(2,3,6-tris(4-methoxyphenyl)-imidazo[2,1-b]thiazol-5-yl)prop-2-en-1-one (11 n):** Yellow solid (149 mg, 74%); mp: 190–194 °C; FT-IR:  $\tilde{\nu}$  = 2354, 1650, 1597, 1252, 1023  $\text{cm}^{-1}$ ;  $^1\text{H NMR}$  (300 MHz,  $\text{CDCl}_3$ ):  $\delta$  = 7.66 (d,  $J$  = 8.68 Hz, 2H), 7.46 (d,  $J$  = 15.67 Hz, 1H), 7.34 (d,  $J$  = 8.68 Hz, 2H), 7.30 (d,  $J$  = 1.7 Hz, 1H), 7.13 (d,  $J$  = 8.87 Hz, 2H), 7.03–6.91 (m, 5H), 6.81–6.2 (m, 3H), 6.51 (d,  $J$  = 15.67 Hz, 1H), 3.92 (s, 3H), 3.87 (s, 3H), 3.86 (s, 3H), 3.77 (s, 3H), 3.75 ppm (s, 3H);  $^{13}\text{C NMR}$  (125 MHz,  $\text{CDCl}_3$ ):  $\delta$  = 187.44, 160.76, 159.72, 159.52, 152.63, 150.65, 150.54, 148.74, 132.16, 131.19, 130.39, 130.22, 129.42, 128.47, 127.33, 126.62, 123.68, 122.43, 121.62, 120.95, 119.51, 114.70, 114.06, 110.45, 109.65, 55.95, 55.85, 55.26, 55.21 ppm; MS (ESI):  $m/z$  633  $[M+H]^+$ ; HRMS (ESI):  $m/z$   $[M+H]^+$  calcd for  $\text{C}_{37}\text{H}_{33}\text{N}_2\text{O}_6\text{S}$ : 633.2053, found: 633.2059.

**(E)-1-(3,4-Dichlorophenyl)-3-(2,3,6-tris(4-methoxyphenyl)imidazo[2,1-b]thiazol-5-yl)prop-2-en-1-one (11 o):** Yellow solid (157 mg, 77%); mp: 188–193 °C; FT-IR:  $\tilde{\nu}$  = 1658, 1575, 1255, 1029, 831  $\text{cm}^{-1}$ ;  $^1\text{H NMR}$  (300 MHz,  $\text{CDCl}_3$ ):  $\delta$  = 7.64 (d,  $J$  = 8.68 Hz, 2H), 7.57 (d,  $J$  = 1.7 Hz, 1H), 7.50 (d,  $J$  = 15.67 Hz, 1H), 7.42 (d,  $J$  = 8.30 Hz, 1H), 7.36 (d,  $J$  = 1.88 Hz, 1H), 7.33 (d,  $J$  = 8.68 Hz, 2H), 7.13 (d,  $J$  = 8.87 Hz, 2H), 7.02 (d,  $J$  = 8.68 Hz, 2H), 6.92 (d,  $J$  = 8.68 Hz, 2H), 6.79 (d,  $J$  = 8.68 Hz, 2H), 6.23 (d,  $J$  = 15.48 Hz, 1H), 3.88 (s, 3H), 3.78 (s, 3H), 3.73 ppm (s, 3H);  $^{13}\text{C NMR}$  (75 MHz,  $\text{CDCl}_3$ ):  $\delta$  = 187.00, 160.84, 160.09, 152.46, 137.89, 136.46, 132.22, 131.20, 130.53, 130.33, 130.07, 128.58, 127.15, 127.07, 126.95, 123.52, 121.48, 121.02, 118.31, 114.73, 114.27, 114.18, 55.39, 55.30 ppm; MS (ESI):  $m/z$  641  $[M+H]^+$ ; HRMS (ESI):  $m/z$   $[M+H]^+$  calcd for  $\text{C}_{35}\text{H}_{27}\text{Cl}_2\text{N}_2\text{O}_4\text{S}$ : 641.1063, found: 641.1070.

**(E)-1-(Pyridin-2-yl)-3-(2,3,6-tris(4-methoxyphenyl)imidazo[2,1-b]thiazol-5-yl)prop-2-en-1-one (11 p):** Yellow solid (102 mg, 56%); mp: 191–194 °C; FT-IR:  $\tilde{\nu}$  = 2832, 1655, 1570, 1251, 1024, 617  $\text{cm}^{-1}$ ;  $^1\text{H NMR}$  (500 MHz,  $\text{CDCl}_3$ ):  $\delta$  = 8.50 (d,  $J$  = 4.27 Hz, 1H), 7.91 (d,  $J$  = 7.78 Hz, 1H), 7.74 (t,  $J$  = 7.62 Hz, 1H), 7.68 (d,  $J$  = 8.69 Hz, 2H), 7.59 (d,  $J$  = 16.02 Hz, 1H), 7.32 (d,  $J$  = 8.54 Hz, 2H), 7.19–7.09 (m, 3H), 7.02–6.96 (m, 3H), 6.87 (d,  $J$  = 8.54 Hz, 2H), 6.78 (d,  $J$  = 8.39 Hz, 2H), 3.86–3.66 ppm (m, 9H);  $^{13}\text{C NMR}$  (125 MHz,  $\text{CDCl}_3$ ):  $\delta$  = 188.89, 160.58, 159.73, 159.48, 154.33, 151.41, 150.95, 148.44, 136.44, 132.15, 130.35, 130.32, 130.25, 128.76, 127.04, 126.41, 126.02, 123.73, 122.33, 121.89, 121.01, 119.76, 114.54, 114.03, 114.01, 55.26, 55.20, 55.12 ppm; MS (ESI):  $m/z$  574  $[M+H]^+$ ; HRMS (ESI):  $m/z$   $[M+H]^+$  calcd for  $\text{C}_{34}\text{H}_{28}\text{N}_3\text{O}_4\text{S}$ : 574.1795, found: 574.1777.

**(E)-3-(6-(4-Chlorophenyl)-2,3-bis(4-methoxyphenyl)imidazo[2,1-b]thiazol-5-yl)-1-(3,4,5-trimethoxyphenyl)prop-2-en-1-one (11 q):** Yellow solid (160 mg, 76%); mp: 214–219 °C; FT-IR:  $\tilde{\nu}$  = 2935, 2833, 1650, 1568, 1260, 827  $\text{cm}^{-1}$ ;  $^1\text{H NMR}$  (500 MHz,  $\text{CDCl}_3$ ):  $\delta$  = 7.67 (d,  $J$  = 8.39 Hz, 2H), 7.44 (d,  $J$  = 8.39 Hz, 2H), 7.37–7.32 (m, 3H), 7.15 (d,  $J$  = 8.69 Hz, 2H), 6.97 (d,  $J$  = 8.69 Hz, 2H), 6.83 (s, 2H), 6.79 (d,  $J$  = 8.69 Hz, 2H), 6.65 (d,  $J$  = 15.56 Hz, 1H), 3.88 (s, 3H), 3.82 (s, 6H), 3.80 (s, 3H), 3.78 ppm (s, 3H);  $^{13}\text{C NMR}$  (75 MHz,  $\text{CDCl}_3$ ):  $\delta$  = 187.26,

160.90, 159.62, 152.77, 150.43, 148.62, 141.91, 134.26, 133.67, 133.18, 132.68, 132.02, 130.44, 130.12, 129.34, 128.84, 128.26, 127.88, 127.27, 123.40, 119.74, 114.88, 114.12, 105.24, 60.83, 56.11, 55.21 ppm; MS (ESI):  $m/z$  667  $[M+H]^+$ ; HRMS (ESI):  $m/z$   $[M+H]^+$  calcd for  $\text{C}_{37}\text{H}_{32}\text{ClN}_2\text{O}_6\text{S}$ : 667.1664, found: 667.1667.

**(E)-3-(6-(4-Chlorophenyl)-2,3-bis(4-methoxyphenyl)imidazo[2,1-b]thiazol-5-yl)-1-(3,4-dimethoxyphenyl)prop-2-en-1-one (11 r):** Yellow solid (142 mg, 71%); mp: 211–213 °C; FT-IR:  $\tilde{\nu}$  = 1652, 1584, 1205, 1026, 838, 695  $\text{cm}^{-1}$ ;  $^1\text{H NMR}$  (300 MHz,  $\text{CDCl}_3$ ):  $\delta$  = 7.67 (d,  $J$  = 8.30 Hz, 2H), 7.44 (d,  $J$  = 8.30 Hz, 2H), 7.36–7.28 (m, 4H), 7.14 (d,  $J$  = 9.06 Hz, 2H), 6.95 (d,  $J$  = 8.30 Hz, 2H), 6.81–6.72 (m, 4H), 6.52 (d,  $J$  = 15.10 Hz, 1H), 3.93 (s, 3H), 3.88 (s, 3H), 3.79 (s, 3H), 3.76 ppm (s, 3H);  $^{13}\text{C NMR}$  (125 MHz,  $\text{CDCl}_3$ ):  $\delta$  = 187.21, 160.86, 159.63, 152.83, 150.55, 148.88, 148.86, 134.24, 133.43, 132.19, 130.98, 130.38, 130.24, 128.95, 128.87, 128.37, 127.13, 123.55, 122.51, 122.04, 120.76, 120.66, 114.79, 114.14, 110.38, 109.74, 56.01, 55.89, 55.30, 55.25 ppm; MS (ESI):  $m/z$  637  $[M+H]^+$ .

**(E)-3-(6-(4-Chlorophenyl)-2,3-bis(4-methoxyphenyl)imidazo[2,1-b]thiazol-5-yl)-1-(3,4-dichlorophenyl)prop-2-en-1-one (11 s):** Yellow solid (161 mg, 79%); mp: 206–210 °C; FT-IR:  $\tilde{\nu}$  = 1654, 1575, 1249, 1027, 827, 702  $\text{cm}^{-1}$ ;  $^1\text{H NMR}$  (500 MHz,  $\text{CDCl}_3$ ):  $\delta$  = 7.65 (d,  $J$  = 8.39 Hz, 2H), 7.57 (d,  $J$  = 1.83 Hz, 1H), 7.46 (d,  $J$  = 8.26 Hz, 2H), 7.43 (t,  $J$  = 3.81 Hz, 2H), 7.34 (d,  $J$  = 1.83 Hz, 1H), 7.32 (d,  $J$  = 8.54 Hz, 2H), 7.13 (d,  $J$  = 8.85 Hz, 2H), 6.92 (d,  $J$  = 8.69 Hz, 2H), 6.80 (d,  $J$  = 8.69 Hz, 2H), 6.21 (d,  $J$  = 15.56 Hz, 1H), 3.79 (s, 3H), 3.73 ppm (s, 3H);  $^{13}\text{C NMR}$  (125 MHz,  $\text{CDCl}_3$ ):  $\delta$  = 186.85, 160.85, 159.74, 151.52, 150.66, 137.58, 136.67, 134.71, 132.98, 132.77, 132.19, 130.62, 130.40, 130.31, 130.05, 129.02, 128.42, 127.52, 127.07, 123.34, 121.74, 120.79, 119.52, 114.72, 114.19, 55.28 ppm; MS (ESI):  $m/z$  645  $[M+H]^+$ ; HRMS (ESI):  $m/z$   $[M+H]^+$  calcd for  $\text{C}_{34}\text{H}_{24}\text{Cl}_3\text{N}_2\text{O}_3\text{S}$ : 645.0567, found: 645.0575.

**(E)-3-(6-(4-Chlorophenyl)-2,3-bis(4-methoxyphenyl)imidazo[2,1-b]thiazol-5-yl)-1-(pyridin-2-yl)prop-2-en-1-one (11 t):** Yellow solid (107 mg, 59%); mp: 192–195 °C; FT-IR:  $\tilde{\nu}$  = 1660, 1574, 1252, 1026, 836, 671  $\text{cm}^{-1}$ ;  $^1\text{H NMR}$  (300 MHz,  $\text{CDCl}_3$ ):  $\delta$  = 8.52 (d,  $J$  = 3.77 Hz, 1H), 7.93 (d,  $J$  = 8.30 Hz, 1H), 7.76 (dt,  $J$  = 7.55, 1.51 Hz, 1H), 7.68 (d,  $J$  = 8.30 Hz, 2H), 7.49 (d,  $J$  = 15.86 Hz, 1H), 7.43–7.29 (m, 5H), 7.17–7.07 (m, 3H), 6.89 (d,  $J$  = 8.30 Hz, 2H), 6.78 (d,  $J$  = 8.30 Hz, 2H), 3.77 (s, 3H), 3.70 ppm (s, 3H);  $^{13}\text{C NMR}$  (125 MHz,  $\text{CDCl}_3$ ):  $\delta$  = 188.73, 160.70, 159.59, 154.10, 150.78, 149.45, 148.56, 136.55, 134.16, 133.14, 132.16, 130.29, 130.23, 129.71, 128.78, 128.59, 126.94, 126.25, 123.59, 122.40, 122.31, 120.82, 114.66, 114.09, 55.23, 55.20 ppm; MS (ESI):  $m/z$  578  $[M+H]^+$ ; HRMS (ESI):  $m/z$   $[M+H]^+$  calcd for  $\text{C}_{33}\text{H}_{25}\text{ClN}_3\text{O}_3\text{S}$ : 578.1299, found: 578.1314.

**(E)-3-(6-(4-Fluorophenyl)-2,3-bis(4-methoxyphenyl)imidazo[2,1-b]thiazol-5-yl)-1-(3,4,5-trimethoxyphenyl)prop-2-en-1-one (11 u):** Yellow solid (166 mg, 78%); mp: 214–217 °C; FT-IR:  $\tilde{\nu}$  = 2980, 2868, 1650, 1570, 1257, 829, 615  $\text{cm}^{-1}$ ;  $^1\text{H NMR}$  (400 MHz,  $\text{CDCl}_3$ ):  $\delta$  = 7.71 (dd,  $J$  = 9.26, 5.89 Hz, 2H), 7.40–7.34 (m, 2H), 7.21–7.14 (m, 4H), 6.98 (d,  $J$  = 8.41 Hz, 2H), 6.84–6.71 (m, 5H), 6.59  $J$  = 15.15 Hz, 1H), 3.91–3.73 ppm (m, 15H);  $^{13}\text{C NMR}$  (75 MHz,  $\text{CDCl}_3$ ):  $\delta$  = 187.35, 161.02, 160.85, 159.59, 152.73, 150.34, 149.068, 141.85, 133.18, 132.66, 131.99, 130.91, 130.12, 129.43, 128.26, 127.10, 121.86, 120.49, 119.45, 115.78, 115.49, 114.82, 114.07, 105.34, 60.80, 56.06, 55.15 ppm; MS (ESI):  $m/z$  651  $[M+H]^+$ ; HRMS (ESI):  $m/z$   $[M+H]^+$  calcd for  $\text{C}_{37}\text{H}_{32}\text{FN}_2\text{O}_6\text{S}$ : 651.1959, found: 651.1964.

**(E)-1-(3,4-Dimethoxyphenyl)-3-(6-(4-fluorophenyl)-2,3-bis(4-methoxyphenyl)imidazo[2,1-b]thiazol-5-yl)prop-2-en-1-one (11 v):** Yellow solid (152 mg, 75%); mp: 207–211 °C; FT-IR:  $\tilde{\nu}$  = 2933, 2834, 1644, 1593, 1268, 1023, 617  $\text{cm}^{-1}$ ;  $^1\text{H NMR}$  (300 MHz,  $\text{CDCl}_3$ ):  $\delta$  = 7.70 (dd,  $J$  = 8.30, 5.28 Hz, 2H), 7.41 (d,  $J$  = 15.86 Hz, 1H), 7.34

(d,  $J=8.30$  Hz, 2H), 7.31 (d,  $J=1.51$  Hz, 1H), 7.20–7.11 (m, 4H), 7.02–6.92 (m, 3H), 6.82–6.71 (m, 3H), 6.50 (d,  $J=15.10$  Hz, 1H), 3.93 (s, 3H), 3.87 (s, 3H), 3.78 (s, 3H), 3.76 ppm (s, 3H);  $^{13}\text{C}$  NMR (125 MHz,  $\text{CDCl}_3$ ):  $\delta=187.22, 160.82, 159.59, 152.76, 150.46, 149.28, 148.83, 132.85, 131.02, 130.93, 130.87, 130.20, 129.01, 128.38, 126.98, 123.54, 122.41, 121.88, 120.78, 120.18, 115.72, 115.55, 114.75, 114.09, 110.37, 109.67, 55.97, 55.85, 55.26, 55.21$  ppm; MS (ESI):  $m/z$  621  $[M+H]^+$ ; HRMS (ESI):  $m/z$   $[M+H]^+$  calcd for  $\text{C}_{36}\text{H}_{30}\text{FN}_2\text{O}_5\text{S}$ : 621.1854, found: 621.1856.

**(E)-1-(3,4-Dichlorophenyl)-3-(6-(4-fluorophenyl)-2,3-bis(4-methoxyphenyl)imidazo[2,1-b]thiazol-5-yl)prop-2-en-1-one**

(**11 w**): Yellow solid (166 mg, 81%); mp: 198–203 °C; FT-IR:  $\tilde{\nu}=1654, 1584, 1251, 1027, 846$   $\text{cm}^{-1}$ ;  $^1\text{H}$  NMR (300 MHz,  $\text{CDCl}_3$ ):  $\delta=7.67$  (dd,  $J=8.30, 5.28$  Hz, 2H), 7.56 (s, 1H), 7.50–7.39 (m, 2H), 7.33 (d,  $J=8.30$  Hz, 3H), 7.19 (d,  $J=8.30$  Hz, 1H), 7.13 (d,  $J=9.06$  Hz, 3H), 6.92 (d,  $J=9.06$  Hz, 2H), 6.79 (d,  $J=9.06$  Hz, 2H), 6.19 (d,  $J=15.10$  Hz, 1H), 3.79 (s, 3H), 3.73 ppm (s, 3H);  $^{13}\text{C}$  NMR (125 MHz,  $\text{CDCl}_3$ ):  $\delta=186.88, 160.12, 152.31, 151.63, 137.71, 136.52, 132.64, 131.91, 131.06, 130.68, 130.48, 130.38, 130.35, 130.04, 129.41, 129.20, 129.04, 128.98, 128.71, 128.61, 127.45, 127.14, 126.89, 121.48, 117.88, 114.25, 55.35$  ppm; MS (ESI):  $m/z$  629  $[M+H]^+$ ; HRMS (ESI):  $m/z$   $[M+H]^+$  calcd for  $\text{C}_{34}\text{H}_{24}\text{Cl}_2\text{FN}_2\text{O}_3\text{S}$ : 629.0863, found: 629.0868.

**(E)-3-(6-(4-Fluorophenyl)-2,3-bis(4-methoxyphenyl)imidazo[2,1-b]thiazol-5-yl)-1-(pyridin-2-yl)prop-2-en-1-one (11 x)**: Yellow solid (95 mg, 52%); mp: 192–196 °C; FT-IR:  $\tilde{\nu}=2922, 1655, 1573, 1251, 1026, 616$   $\text{cm}^{-1}$ ;  $^1\text{H}$  NMR (400 MHz,  $\text{CDCl}_3$ ):  $\delta=8.52$  (d,  $J=4.24$  Hz, 1H), 7.93 (d,  $J=7.63$  Hz, 1H), 7.79–7.65 (m, 3H), 7.51 (d,  $J=15.26$  Hz, 1H), 7.39–7.31 (m, 3H), 7.17–7.06 (m, 5H), 6.90 (d,  $J=8.48$  Hz, 2H), 6.79 (d,  $J=8.48$  Hz, 2H), 3.77 (s, 3H), 3.72 ppm (s, 3H);  $^{13}\text{C}$  NMR (75 MHz,  $\text{CDCl}_3$ ):  $\delta=187.88, 160.70, 154.15, 149.93, 148.54, 148.07, 136.52, 132.63, 132.16, 130.91, 130.78, 130.24, 129.83, 129.54, 128.76, 128.64, 126.02, 122.39, 122.18, 120.84, 120.32, 115.72, 115.43, 114.68, 114.09, 55.18$  ppm; MS (ESI):  $m/z$  562  $[M+H]^+$ ; HRMS (ESI):  $m/z$   $[M+H]^+$  calcd for  $\text{C}_{33}\text{H}_{25}\text{FN}_3\text{O}_3\text{S}$ : 562.1595, found: 562.1589.

## Biology

### Anticancer activity

The cytotoxic activities of the compounds were determined using an MTT assay.<sup>[40–41]</sup> Cells were seeded at  $1 \times 10^4$  cells/well in Dulbecco's modified Eagle's medium (DMEM) (200  $\mu\text{L}$ ), supplemented with 10% fetal bovine serum (FBS) in each well of 96-well microculture plates, and incubated for 24 h at 37 °C in a  $\text{CO}_2$  incubator. Compounds, diluted to the desired concentrations in culture medium, were added to the wells with respective vehicle control. After 48 h of incubation, 3-(4, 5-dimethylthiazol-2-yl)-2,5-diphenyl tetrazolium bromide (MTT) (10  $\mu\text{L}$ , 5  $\text{mg mL}^{-1}$ ) was added to each well, and the plates were further incubated for 4 h. Then the supernatant from each well was carefully removed, formazan crystals were dissolved in DMSO (100  $\mu\text{L}$ ), and absorbance at 540 nm wavelength was recorded. Three independent experiments were performed in triplicate.

### Cell-cycle analysis

Fluorescence-activated cell sorting (FACS) was performed to evaluate the distribution of the cells through the cell-cycle phases. A549 lung cancer cells were incubated with compound **11 x** at 0.25, 0.5 and 1  $\mu\text{M}$  for 24 h. Untreated and treated cells were harvested, washed with phosphate-buffered saline (PBS), fixed in ice-cold

70% EtOH, and stained with propidium iodide (PI; Sigma–Aldrich). Cell-cycle phase determination was performed by flow cytometry (Becton Dickinson FACS Caliber) as previously described.<sup>[55]</sup> Two independent experiments were performed in triplicate. Statistical analysis was performed using GraphPad Prism software version 5.01.

### Tubulin polymerization assay

A fluorescence-based in vitro tubulin polymerization assay was performed according to the manufacturer's protocol (cat. no. BK011; Cytoskeleton, Inc., Denver, CO, USA). The reaction mixture (total volume of 10  $\mu\text{L}$ ) contained PEM buffer (80 mM piperazine-*N,N'*-bis(2-ethanesulfonic acid) (PIPES), 0.5 mM EDTA, 2 mM  $\text{MgCl}_2$ , pH 6.9) and guanosine-5'-triphosphate (GTP; 1  $\mu\text{M}$ ) in the presence or absence of test compound (final concentration of 3  $\mu\text{M}$ ). Tubulin polymerization was followed by a time-dependent increase in fluorescence due to the incorporation of a fluorescence reporter into microtubules as polymerization proceeds. Fluorescence emission at 420 nm (excitation wavelength at 360 nm) was measured by using a Varioscan multimode plate reader (Thermo Scientific Inc.). Nocodazole was used as positive control in each assay. The  $\text{IC}_{50}$  value was defined as the compound concentration required to inhibit 50% of tubulin assembly compared to the untreated control. The reaction mixture for these experiments included: tubulin (3  $\text{mg mL}^{-1}$ ) in PEM buffer and GTP (1  $\mu\text{M}$ ) in the presence or absence of test compound (2.5, 5, 10, and 15  $\mu\text{M}$ ). Polymerization was monitored by increase in the fluorescence as mentioned above at 37 °C.<sup>[43,44]</sup> Two independent experiments were performed in triplicate. Statistical analysis was performed using GraphPad Prism software version 5.01.

### Colchicine competition assay

Test compound (**11 x**) (5  $\mu\text{M}$ , 10  $\mu\text{M}$ , 15  $\mu\text{M}$ , and 10  $\mu\text{M}$ ) was co-incubated with colchicine (4  $\mu\text{M}$ ) in Tris buffer (30 mM, pH 6.9) containing tubulin (3  $\mu\text{M}$ ) for 60 min at 37 °C. Nocodazole was used as a positive control, whereas paclitaxel was used as the negative control, which does not bind at the colchicine site. After incubation, the fluorescence of the tubulin–colchicine complex was determined by using a Tecan multimode reader (excitation wavelength at 350 nm and emission wavelength at 435 nm). Tris buffer (30 mM, pH 6.9) was used as a blank; the fluorescence was subtracted from all other results. Fluorescence values were normalized to the DMSO control.<sup>[56]</sup> Two independent experiments were performed in duplicate.

### Immunohistochemistry

A549 cells were seeded on glass cover slips, incubated for 24 h in the presence or absence of test compound **11 x** (0.5 and 1  $\mu\text{M}$ ) for 24 h. Following the termination of incubation, cells were permeabilized with 0.5% Triton X100 in microtubule stabilizing buffer (0.1 M PIPES, 2 mM  $\text{MgCl}_2$ , 1 mM ethylene glycol tetraacetic acid (EGTA), 4% polyethylene glycol, pH 6.8) and fixed with 3.7% paraformaldehyde for 20 min in the same buffer. Later, cover slips were blocked with 1% bovine serum albumin (BSA) in PBS for 1 h followed by incubation with a primary anti-tubulin (mouse monoclonal) antibody and FITC-conjugated secondary mouse anti-IgG antibody. Photographs were taken using the fluorescence microscope, equipped with FITC settings, and the pictures were analyzed for the integrity of the microtubule network. In parallel experiments, nocodazole (1  $\mu\text{M}$ ) was used as a positive control for analyzing microtubule integrity.<sup>[44]</sup>

### Hoechst staining

Cells were seeded at a density of  $1 \times 10^4$  over 18 mm cover slips and incubated for 24 h. After incubation, cells were treated with **11x** (0.5 and  $1 \mu\text{M}$ ) for 24 h. Hoechst 33258 (Sigma–Aldrich) ( $0.5 \text{ mg mL}^{-1}$ ) was added to the cells, and the cover slips were incubated for 30 min at  $37^\circ\text{C}$ . Later, cells were washed with PBS. Cells from each cover slip were captured from randomly selected fields under a fluorescent microscope (Leica, Germany) to qualitatively determine the proportion of viable and apoptotic cells based on their relative fluorescence and nuclear fragmentation.<sup>[57]</sup>

### Caspase-3 activity

Caspase-3 assay was conducted for detection of apoptosis in A549 cells. The commercially available apoptosis detection kit (caspase-3 colorimetric assay kit, Sigma) was used. A549 cells were treated with compound **11x** (0.5 and  $1 \mu\text{M}$ ) for 48 h. After 48 h of treatment, cells were collected by centrifugation (12000 rpm, 15 min,  $4^\circ\text{C}$ ), washed once with PBS, and cell pellets were collected. The cell pellet was suspended in lysis buffer and incubated for 15 min. After incubation, cells were centrifuged at 20000 rpm for 15 min at  $4^\circ\text{C}$ , and the supernatant was collected. Supernatants were used for measuring caspase-3 activity using an enzyme-linked immunosorbent assay (ELISA), according to the manufacturer's instructions. Two independent experiments were performed in triplicate. Statistical analysis was performed using GraphPad Prism software version 5.01.

### Flow cytometric evaluation of apoptosis

A549 cells ( $1 \times 10^6$ ) were seeded in six-well plates and allowed to grow overnight. The medium was then replaced with complete medium containing **11x** (0.5 and  $1 \mu\text{M}$ ) for 24 h along with vehicle alone (0.001% DMSO) as control. After 24 h of drug treatment, cells from the supernatant and adherent monolayer cells were harvested by trypsinization, washed with PBS, and centrifuged at 3000 rpm (5 min,  $4^\circ\text{C}$ ). Then the cells ( $1 \times 10^6$ ) were stained with Annexin V–FITC and PI using the Annexin V–PI apoptosis detection kit (Invitrogen). Flow cytometry was performed using a FACScan (Becton Dickinson) equipped with a single 488 nm argon laser as described earlier.<sup>[58]</sup> Annexin V–FITC was analyzed using excitation and emission settings of 488 nm and 535 nm (FL-1 channel); PI, 488 nm and 610 nm (FL-2 channel). Debris and clumps were gated out using forward and orthogonal light scatter.

### DNA fragmentation analysis

Cells were seeded ( $1 \times 10^6$ ) in six-well plates and incubated for 24 h. After incubation, cells were treated with compound **11x** (0.25, 0.5, and  $1 \mu\text{M}$ ) for 24 h. After 24 h of treatment, cells were collected and centrifuged at 2500 rpm for 5 min at  $4^\circ\text{C}$ . The pellet was collected and washed with PBS. Lysis buffer ( $100 \mu\text{L}$ ) was added. Cells were centrifuged at 3000 rpm for 5 min at  $4^\circ\text{C}$ , and the supernatant was collected. Sodium dodecyl sulfate (SDS) ( $10 \mu\text{L}$  of 10% solution) and RNase-A ( $10 \mu\text{L}$ ,  $50 \text{ mg mL}^{-1}$ ) were added, and the solution was incubated for 2 h at  $56^\circ\text{C}$ . After that, proteinase K ( $10 \mu\text{L}$ ,  $25 \text{ mg mL}^{-1}$ ) was added, and the solution was incubated at  $37^\circ\text{C}$  for 2 h. After incubation, ammonium acetate ( $65 \mu\text{L}$  of 10 M) and ice-cold EtOH ( $500 \mu\text{L}$ ) were added and mixed well. This sample was incubated at  $-80^\circ\text{C}$  for 1 h. After that samples were centrifuged at 12000 rpm for 20 min at  $4^\circ\text{C}$  and washed with 80% EtOH followed by air drying for 10 min at RT. The pellet was dis-

solved in Tris-EDTA (TE) buffer ( $50 \mu\text{L}$ , pH 7.4). After that, DNA laddering was determined by 2% agarose gel electrophoresis.<sup>[59]</sup>

### Protein extraction and Western blot analysis

A549 cells were treated with compound **11x** (0.5 and  $1 \mu\text{M}$ ) for 48 h. Cells were lysed in ice-cold radioimmunoprecipitation assay (RIPA) buffer ( $1 \times \text{PBS}$ , 1% NP-40 detergent, 0.5% sodium deoxycholate, and 0.1% SDS) containing phenylmethanesulfonyl fluoride (PMSF) ( $100 \text{ mg mL}^{-1}$ ), aprotinin ( $5 \text{ mg mL}^{-1}$ ), leupeptin ( $5 \text{ mg mL}^{-1}$ ), pepstatin ( $5 \text{ mg mL}^{-1}$ ), and NaF ( $100 \text{ mg mL}^{-1}$ ). After centrifugation at 12000 rpm for 10 min, the protein in the supernatant was quantified by the Bradford method (BIO-RAD) by using a multimode Varioskan instrument (Thermo Fischer Scientific Ltd.). Protein ( $50 \text{ mg}$  per lane) was loaded in a 12% SDS polyacrylamide gel. After electrophoresis, the protein was transferred to a polyvinylidene difluoride (PVDF) membrane (Thermo Scientific Inc.). The membrane was blocked at RT for 2 h in Tris-buffered saline (TBS) with 0.1% Tween 20 (TBST) containing 5% blocking powder (Santa Cruz). The membrane was washed with TBST for 5 min, then primary antibody was added, and the membrane was incubated at  $4^\circ\text{C}$  overnight. Bcl-2, Bax, and  $\beta$ -actin antibodies were purchased from Cell Signaling Technology (CST). The membrane was incubated with the corresponding horseradish-peroxidase-labeled secondary antibody (1:2000; CST) at RT for 1 h. Membranes were washed with TBST three times for 15 min, and the blots were visualized with chemiluminescence reagent (Thermo Fischer Scientific Ltd). Images were captured by using the UVP ChemiDoc imager (BIO-RAD).<sup>[60]</sup>

### Molecular docking procedure

The optimizations of all the compounds were carried out in Gaussian 09 using PM3 semi-empirical method.<sup>[61]</sup> The tubulin–colchicine–soblidotin cocrystal structure was downloaded from the RSCB Protein Data Bank (PDB ID: 3E22).<sup>[62]</sup> AutoDock 4.2 software<sup>[63]</sup> was used to perform the docking studies. The visualization and analysis of interactions was performed using Pymol, version 0.99.<sup>[64]</sup>

### Acknowledgements

M.B.K. and S.F. thank the University Grants Commission (UGC), New Delhi (India) for the research fellowships. The authors also thank the Indian Council of Scientific and Industrial Research (CSIR) for financial support under the 12th five-year plan project "Affordable Cancer Therapeutics (ACT)" (CSC0301).

**Keywords:** antiproliferation • apoptosis • cell-cycle arrest • chalcones • molecular docking • tubulin polymerization

- [1] a) A. L. Risinger, F. J. Giles, S. L. Mooberry, *Cancer Treat. Rev.* **2009**, *35*, 255–261; b) R. O. Carlson, *Expert Opin. Invest. Drugs* **2008**, *17*, 707–722.
- [2] K. H. Downing, E. Nogales, *Curr. Opin. Cell Biol.* **1998**, *10*, 16–22.
- [3] R. J. Toso, M. A. Jordan, K. W. Farrel, B. Matsumato, L. Wilson, *Biochemistry* **1993**, *32*, 1285–1293.
- [4] C. M. Lin, H. H. Ho, G. R. Pettit, E. Hamel, *Biochemistry* **1989**, *28*, 6984–6991.
- [5] T. Beckers, S. Mahboobi, *Drugs Future* **2003**, *28*, 767–785.
- [6] J. C. Medina, J. Houze, D. L. Clark, S. Schwendner, H. Beckmann, B. Shan, *Abstracts of Papers*, 222nd American Chemical Society National Meeting, Chicago, August 26–30, **2001**; ACS: Washington, DC.
- [7] E. A. Perez, *Mol. Cancer Ther.* **2009**, *8*, 2086–2095.

- [8] F. D. Boyer, J. Dubois, S. Thoret, M. E. T. H. Dau, I. Hanna, *Bioorg. Chem.* **2010**, *38*, 149–158.
- [9] M. N. Semenova, A. S. Kiselyov, D. V. Tsyganov, L. D. Konyushkin, S. I. Firganga, R. V. Semenov, O. R. Malyshev, M. M. Raihstat, F. Fuchs, A. Stielow, M. Lantow, A. A. Philchenkov, M. P. Zavelevich, N. S. Zefirov, S. A. Kuznetsov, V. V. Semenov, *J. Med. Chem.* **2011**, *54*, 7138–7149.
- [10] B. L. Flynn, G. S. Gill, D. W. Grobelny, J. H. Chaplin, D. Paul, A. F. Leske, T. C. Lavranos, D. K. Chalmers, S. A. Charman, E. Kostewicz, D. M. Shackelford, J. Morizzi, E. Hamel, M. K. Jung, G. Kremmidiotis, *J. Med. Chem.* **2011**, *54*, 6014–6027.
- [11] Q. Zhang, Y. Peng, X. I. Wang, S. M. Keenan, S. Arora, W. J. Welsh, *J. Med. Chem.* **2007**, *50*, 749–754.
- [12] G. R. Pettit, C. R. Anderson, D. L. Herald, M. K. Jung, D. J. Lee, E. Hamel, R. K. Pettit, *J. Med. Chem.* **2003**, *46*, 525–531.
- [13] R. Romagnoli, P. G. Baraldi, T. Sarkar, M. D. Carrion, C. L. Cara, O. Cruz-Lopez, D. Preti, M. A. Tabrizi, M. Tolomeo, S. Grimaudo, A. Di Cristina, N. Zonta, J. Balzarini, A. Brancale, H. P. Hsieh, E. Hamel, *J. Med. Chem.* **2008**, *51*, 1464–1468.
- [14] R. R. Dangi, N. Hussain, G. L. Talesara, *Med. Chem. Res.* **2011**, *20*, 1490–1498.
- [15] T. Juspin, M. Laget, T. Terme, N. Azas, P. Vanelle, *Eur. J. Med. Chem.* **2010**, *45*, 840–845.
- [16] N. U. Güzeldemirci, Ö. Kucükbasmaci, *Eur. J. Med. Chem.* **2010**, *45*, 63–68.
- [17] N. S. Shetty, R. S. Koti, R. S. Lamani, N. P. Badiger, I. A. M. Khazi, *J. Sulfur Chem.* **2008**, *29*, 539–547.
- [18] R. S. Lamani, N. S. Shetty, R. R. Kamble, I. A. M. Khazi, *Eur. J. Med. Chem.* **2009**, *44*, 2828–2833.
- [19] V. B. Jadhav, M. V. Kulkarni, V. P. Rasal, S. S. Biradar, M. D. Vinay, *Eur. J. Med. Chem.* **2008**, *43*, 1721–1729.
- [20] R. Budriesi, P. Ioan, A. Locatelli, S. Cosconati, A. Leoni, M. P. Ugenti, A. Andreani, R. di Toro, A. Bedini, S. Spampinato, L. Marinelli, E. Novellino, A. Chiarini, *J. Med. Chem.* **2008**, *51*, 1592–1600.
- [21] A. Kamal, D. Dastagiri, M. J. Ramaiah, J. S. Reddy, E. V. Bharathi, C. Srinivas, S. N. C. V. L. Pushpavalli, D. Pal, M. Pal-Bhadra, *ChemMedChem* **2010**, *5*, 1937–1947.
- [22] A. Kamal, J. S. Reddy, M. J. Ramaiah, D. Dastagiri, E. V. Bharathi, M. V. Premasagar, S. N. C. V. L. Pushpavalli, D. Pal, P. Roy, M. Pal-Bhadra, *MedChemComm* **2010**, *1*, 355–360.
- [23] A. Andreani, S. Burnelli, M. Granaola, A. Leoni, A. Locatelli, R. Morigi, M. Rambaldi, L. Varoli, N. Calonghi, C. Cappadone, M. Voltattorni, M. Zini, C. Stefanelli, L. Masotti, R. H. Shoemaker, *J. Med. Chem.* **2008**, *51*, 7508–7513.
- [24] A. Andreani, S. Burnelli, M. Granaola, A. Leoni, A. Locatelli, R. Morigi, M. Rambaldi, L. Varoli, N. Calonghi, C. Cappadone, G. Farruggia, M. Zini, C. Stefanelli, L. Masotti, N. S. Radin, R. H. Shoemaker, *J. Med. Chem.* **2008**, *51*, 809–816.
- [25] a) S. Cheenpracha, C. Karalai, C. Ponglimanont, S. Subhadhiraakul, S. Tewtrakul, *Bioorg. Med. Chem.* **2006**, *14*, 1710–1714; b) O. Nerya, R. Musa, S. Khatib, S. Tamir, J. Vaya, *Phytochemistry* **2004**, *65*, 1389–1395; c) Z. Nowakowska, *Eur. J. Med. Chem.* **2007**, *42*, 125–137; d) M. L. Go, X. Wu, X. L. Liu, *Curr. Med. Chem.* **2005**, *12*, 483–499; e) P. M. Sivakumar, S. Ganesan, P. Veluchamy, M. Doble, *Chem. Biol. Drug Des.* **2010**, *76*, 407–411; f) A. C. Waiss, R. E. Lundin, D. J. Stern, *Tetrahedron Lett.* **1964**, *5*, 513–518.
- [26] T. Sakai, R. N. Eskander, Y. Guo, K. J. Kim, J. Mefford, J. Hopkins, N. N. Bhatia, X. Zi, B. H. Hoang, *J. Orthop. Res.* **2012**, *30*, 1045–1050.
- [27] R. Nishimura, K. Tabata, M. Arakawa, Y. Ito, Y. Kimura, T. Akihisa, H. Nagai, A. Sakuma, H. Kohno, T. Suzuki, *Biol. Pharm. Bull.* **2007**, *30*, 1878–1883.
- [28] E. Hijova, *Bratisl. Lek. Listy* **2006**, *107*, 80–84.
- [29] H. J. Zhang, Y. Qian, D. D. Zhu, X. G. Yang, H. L. Zhu, *Eur. J. Med. Chem.* **2011**, *46*, 4702–4708.
- [30] P. Singh, M. Kaur, W. Holzer, *Eur. J. Med. Chem.* **2010**, *45*, 4968–4982.
- [31] A. Kamal, Y. V. Srikanth, M. N. Khan, T. B. Shaik, M. Ashraf, *Bioorg. Med. Chem. Lett.* **2010**, *20*, 5229–5231.
- [32] A. Kamal, F. Sultana, M. J. Ramaiah, Y. V. V. Srikanth, A. Viswanath, C. Kishore, P. Sharma, S. N. Pushpavalli, A. Addlagatta, M. Pal-Bhadra, *ChemMedChem* **2012**, *7*, 292–300.
- [33] A. Kamal, S. Faazil, J. Ramaiah, Md. Ashraf, M. B. Krishna, S. N. Pushpavalli, N. Patel, M. Pal-Bhadra, *Bioorg. Med. Chem. Lett.* **2013**, *23*, 5733–5739.
- [34] A. Kamal, V. S. Reddy, S. Karnewar, S. S. Chourasiya, A. B. Shaik, G. B. Kumar, C. Kishore, M. K. Reddy, M. P. N. Rao, A. Nagabhushana, K. V. S. R. Krishna, A. Addlagatta, S. Kotamraju, *ChemMedChem* **2013**, *8*, 2015–2025.
- [35] C. Kanthou, O. Greco, A. Stratford, I. Cook, R. Knight, O. Benzakour, G. Tozer, *Am. J. Pathol.* **2004**, *165*, 1401–1411.
- [36] S. Chiba, L. Zhang, G. Y. Ang, B. W. Q. Hui, *Org. Lett.* **2010**, *12*, 2052–2055.
- [37] T. Mase, H. Arima, K. Tomioka, T. Yamada, K. Murse, *J. Med. Chem.* **1986**, *29*, 386–394.
- [38] A. U. Siddiqui, V. U. M. Roa, M. Maimirani, A. H. Siddiqui, *J. Heterocycl. Chem.* **1995**, *32*, 353–356.
- [39] F. Herencia, M. L. Ferrndiz, A. Ubeda, J. N. Domnguez, J. E. Charris, G. Lobo, M. J. Alcaraz, *Bioorg. Med. Chem. Lett.* **1998**, *8*, 1169–1174.
- [40] Á. Berényi, R. Minorics, Z. Iványi, I. Ocsosvzki, E. Duczaa, H. Thole, J. Messinger, J. Wöfling, G. Mótyán, E. Merynák, E. Frank, G. Schneider, I. Zupkó, *Steroids* **2013**, *78*, 69–78.
- [41] a) B. Das, C. R. Reddy, J. Kashanna, S. K. Mamidyalu, C. G. Kumar, *Med. Chem. Res.* **2012**, *21*, 3321–3325; b) T. Mosmann, *J. Immunol. Methods* **1983**, *65*, 55–63.
- [42] A. Jordan, J. A. Hadfield, N. J. Lawrence, A. T. McGown, *Med. Res. Rev.* **1998**, *18*, 259–296.
- [43] K. Huber, P. Patel, L. Zhang, H. Evans, A. D. Westwell, P. M. Fischer, S. Chan, S. Martin, *Mol. Cancer Ther.* **2008**, *7*, 143–151.
- [44] A. Kamal, Y. V. V. Srikanth, T. B. Shaik, M. N. A. Khan, M. Ashraf, M. K. Reddy, K. A. Kumar, S. V. Kalivendi, *MedChemComm* **2011**, *2*, 819–823.
- [45] Z. L. Liu, W. Tian, Y. Wang, S. Kuang, X. M. Luo, Q. Yu, *Acta Pharmacol. Sin.* **2012**, *33*, 261–270.
- [46] L. M. Leoni, E. Hamel, D. Genini, H. Shih, C. J. Carrera, H. B. Cottam, D. A. Carson, *J. Natl. Cancer Inst.* **2000**, *92*, 217–224.
- [47] E. Pasquier, M. Kavallaris, *IUBMB Life* **2008**, *60*, 165–170.
- [48] L. H. Zhang, L. Wu, H. K. Raymon, R. S. Chen, L. Corral, M. A. Shirley, R. K. Narla, J. Gamez, G. W. Muller, D. I. Stirling, B. J. Bartlett, P. H. Schafer, F. Payvandi, *Cancer Res.* **2006**, *66*, 951–959.
- [49] N. M. Weir, K. Selvendiran, V. K. Kutala, L. Tong, S. Vishwanath, M. Rajaram, S. Tridandapani, S. Anant, P. Kuppusamy, *Cancer Biol. Ther.* **2007**, *6*, 178–184.
- [50] S. Iyer, D. J. Chaplin, D. S. Rosenthal, A. H. Boulares, L. Y. Li, M. E. Smulson, *Cancer Res.* **1998**, *58*, 4510–4514.
- [51] H. Zhu, J. Zhang, N. Xue, Y. Hu, B. Yang, Q. He, *Invest. New Drugs* **2010**, *28*, 493–501.
- [52] S. M. Konstantinov, M. R. Berger, *Cancer Lett.* **1999**, *144*, 153–160.
- [53] A. H. Wyllie, *Br. Med. Bull.* **1997**, *53*, 451–465.
- [54] B. Antonsson, *Mol. Cell. Biochem.* **2004**, *256–257*, 141–155.
- [55] M. Szumilak, A. Szulawska-Mroczek, K. Koprowska, M. Stasiak, W. Lewgond, A. Stanczak, M. Czyz, *Eur. J. Med. Chem.* **2010**, *45*, 5744–5751.
- [56] M. I. Brett, L. Luca, A. Esther, J. O. C. Cornelius, S. T. Yaw, M. L. D. Huw, Mc. Grahame, R. V. Ashok, R. S. David, *Nat. Commun.* **2014**, *5*, 3155.
- [57] R. Shankar, B. Chakravarti, U. S. Singh, M. I. Ansari, S. Deshpande, S. K. D. Dwivedi, H. K. Bid, R. Konwar, G. Kharkwal, V. Chandra, A.; Dwivedi, K. Hajela, *Bioorg. Med. Chem.* **2009**, *17*, 3847–3856; Dwivedi, K. Hajela, *Bioorg. Med. Chem.* **2009**, *17*, 3847–3856.
- [58] a) L. J. Browne, (Ciba Geigy AG, Basel, Switzerland), *Eur. Pat. Appl. ZA8403677 A*, **1985**; [*Chem. Abstr.* **1986**, *105*, 6507d]; b) L. J. Browne, C. Gude, H. Rodriguez, R. E. Steele, A. Bhatnager, *J. Med. Chem.* **1991**, *34*, 725–736.
- [59] A. Kamal, G. R. Krishna, V. L. Nayak, P. Raju, A. V. S. Rao, A. Viswanath, M. V. P. S. Vishnuvardhan, S. Ramakrishna, G. Srinivas, *Bioorg. Med. Chem.* **2012**, *20*, 789–800.
- [60] A. Kamal, N. V. S. Reddy, V. L. Nayak, V. S. Reddy, B. Prasad, V. D. Nimbarde, V. Srinivasulu, M. V. P. S. Vishnuvardhan, C. S. Reddy, *ChemMedChem* **2014**, *9*, 117–128.
- [61] Gaussia 09 (Revision B.1), M. J. Frisch, G. W. Trucks, H. B. Schlegel, G. E. Scuseria, G. A. Robb, J. R. Cheeseman, G. Scalmani, V. Barone, B. Menucci, M. A. Petersson, H. Nakatsuji, M. Caricato, X. Li, H. P. Hratchian, A. F. Izmaylov, J. Bloino, G. Zheng, J. L. Sonnenberg, M. Hada, M. Ehara, K. Toyota, R. Fukuda, J. Hasegawa, M. Ishida, T. Nakajima, Y. Honda, O. Kitao, H. Nakai, T. Vreven, J., J. A. Montgomery, J. E. Peralta, F. Ogliaro, M. Bearpark, J. J. Heyd, E. Brothers, K. N. Kudin, V. N. Staroverov, R. Kobayashi, J. Normand, K. Raghavachari, A. Rendell, J. C. Burant, S. S. Iyengar, J. Tomasi, M. Cossi, N. Rega, J. M. Millam, M. Klene, J. E. Knox, J. B.

- Cross, V. Bakken, C. Adamo, J. Jaramillo, R. Gomperts, R. E. Stratmann, O. Yazyev, A. J. Austin, R. Cammi, C. Pomelli, J. W. Ochterski, R. L. Martin, K. Morokuma, V. G. Zakrzewski, G. A. Voth, P. Salvador, J. J. Dannenberg, S. Dapprich, A. D. Daniels, Ö. Farkas, J. B. Foresman, J. V. Ortiz, J. Cioslowski, D. J. Fox, Gaussian, Inc., Wallingford CT. **2010**.
- [62] A. Cormier, M. Marchand, R. B. G. Ravelli, M. Knossow, B. Gigant, *EMBO Rep.* **2008**, *9*, 1101–1106.
- [63] AutoDock, version 4.2, **2009**; Homepage: <http://autodock.scripps.edu>; Reference: G. M. Morris, R. Huey, W. Lindstrom, M. F. Sanner, R. K. Belew, D. S. Goodsell, A. J. Olson, *J. Comp. Chem.* **2009**, *16*: 2785–2791.
- [64] The PyMOL Molecular Graphics System, Version 1.5.0.4 Schrödinger, LLC.
- [65] A. Massarotti, A. Coluccia, R. Silvestri, G. Sorba, A. Brancale, *ChemMedChem* **2012**, *7*, 33–42.

---

Received: July 25, 2014

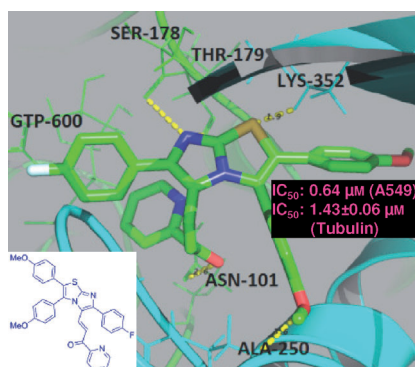
Published online on ■ ■ ■, 0000

## FULL PAPERS

A. Kamal,\* M. Balakrishna, V. L. Nayak,  
T. B. Shaik, S. Faazil, V. D. Nimbarde



### Design and Synthesis of Imidazo[2,1-*b*]thiazole–Chalcone Conjugates: Microtubule-Destabilizing Agents



**Destabilizing microtubules:** Chalcone-containing imidazo[2,1-*b*]thiazole scaffolds were designed, synthesized, and evaluated for their cytotoxic activity. The new compounds had promising cytotoxic activity but one in particular showed potent antiproliferative activity towards the A549 lung cancer cell line. This compound was shown to inhibit microtubule assembly, induce cell-cycle arrest, and lead to apoptosis. Molecular modeling and competitive binding experiments indicate that compound **11 x** binds at the colchicine binding site on tubulin.